We thank the referees for their insightful comments. Our point-by-point responses to the comments and the revisions to the manuscript are as follows:

Anonymous Referee #1
Received and published: 16 July 2020

Shah et al. report global predictions of cloud and precipitation acidity from an updated version of GEOS-CHEM. The addition of formic and acetic acids and of dust enable the model to better capture regionally important influences on hydrometeor pH and to better match spatial variations in acidity relative to other recent model predictions. The work is thorough, carefully conducted and, for the most part, clearly explained. I have a few comments and suggestions:

1. abstract, lines 21-22: please clarify that the model successfully reproduces annual mean rainwater pH observations.
We have clarified in the abstract of the revised manuscript that the model reproduces annual mean observations.

2. The authors refer to rainwater acidity and go to the trouble of somewhat strangely defining rainwater to include snow. Why not just use the more general term "precipitation" throughout?
Following the referee's suggestion, we now use the term "precipitation" instead of "rainwater" throughout the manuscript.

3. The addition of formic and acetic acids captures important influences on cloud and precipitation acidity. a. it would be useful to mention that future work might also warrant consideration of other key dicarboxylic acids (e.g., oxalic, succinic) that can be abundant in clouds. b. I was disappointed to see the authors recognize their new scheme continues to significantly underpredict acetic acid concentrations, as evidenced by comparison to source strengths considered by others as well as observed wet deposition fluxes (a factor of 4) but did not take action to correct for this discrepancy. They point out that a biogenic emissions scaling could correct this discrepancy similar to how they corrected for HCOOH underpredictions. Why not make that correction as part of this paper?
We did not attempt to correct the model underestimate of CH_3COOH as its effect on pH is small. We have clarified this further and emphasized the need to better understand the sources of carboxylic acids with the following additions:
On page 5, line 18 (underlined part added):
  "model CH_3COOH could be corrected similarly to HCOOH in future work by scaling up biogenic emission. But the effect is relatively small. We find in the model that the global mean cloudwater pH would decrease by 0.05 units if we increased CH_3COOH concentrations by a factor of 4."
And on page 13, line 24 we have added:
  "Carboxylic acids affect cloudwater and precipitation pH globally, but their sources are uncertain. Our simulation could reproduce the observed HCOOH wet deposition flux by using scaled-up biogenic emissions but underestimated CH_3COOH flux by a factor of 4, indicating that a better understanding of their sources is needed. Dicarboxylic acids, such as oxalic, succinic, and malonic acids, are also present in cloudwater and precipitation and their effect on pH needs to be evaluated."

4. Eq'n. 1: The authors exclude both CO32- and OH- from this charge balance equation, arguing that both are small for pH<8. I am OK with this omission of CO32- but worry about artifacts in their higher pH simulations due to omission of OH-. At pH 7, for example [OH-] equals [H+], meaning that omission of OH- introduces a relatively significant error in the H+ concentration obtained from eq'n 1 in this pH range. Why not just include OH- and eliminate this high pH artifact? How does this artifact of OH- omission at high pH influence the comparison with other cloud models at high pH (e.g., p.9, lines 59+)

The omission of $[OH^-]$ in Eq. (1) incurs a negligible bias. We have clarified this in the text on page 9 as follows (underlined text added):

"$\overline{[HCO_3^-]}$ is calculated from equilibrium with atmospheric CO_2 as follows:

$$\overline{[HCO_3^-]} = \frac{H_{CO_2} K_{c1} P_{CO_2}}{\overline{[H^+]}} \qquad (4)$$

where H_{CO_2} and K_{c1} are the Henry's law coefficient for CO_2 and the $CO_2(aq)/HCO_3^-$ acid dissociation constant, respectively, at the average cloudwater temperature for the period and domain (Tables 1 and 2). P_{CO_2} is the CO_2 partial pressure, taken to be 390 ppm as representative of 2013. Substituting these values in Eq. (4), $\overline{[HCO_3^-]} \approx 10^{-11.3}/\overline{[H^+]}$. Over the range of cloudwater pH values (3–8.5), $\overline{[CO_3^{2-}]}$ $\left(\approx 10^{-21.6}/\overline{[H^+]}^2 \right)$ and $\overline{[OH^-]}$ $\left(\approx 10^{-14}/\overline{[H^+]} \right)$ are negligible compared to $\overline{[HCO_3^-]}$ and omitted from Eq. (1) (Stumm et al., 1987)."

5. The authors discuss the importance of NH4+ and carboxylic acid buffering on cloud pH when strong acid inputs decrease. It would be good to mention here that other buffers may also play an important role, including HCO3- (see, e.g., Collett et al. (1999) Internal acid buffering in San Joaquin Valley fog drops and its influence on aerosol processing. Atmos. Environ., 33, 4833-4847).

We include this now on page 9, line 30 in the revised manuscript:

"Buffering by CO_2 and SO_2 becomes important at pH values above 6 (Liljestrand, 1985) and buffering by higher organic acids is important in highly polluted areas (Collett et al., 1999)."

6. p. 13, lines 89-92: Again talking about the pH buffering effect, the authors point out that a factor of 2 decrease in sulfate and nitrate inputs yields a pH increase of 1 unit, with buffering, vs. 2.1 units predicted w/o buffering. Have they examined historical time series of cloud pH to see if this effect is apparent in ambient observations? One simple comparison to ballpark this might be to look at the pH trends over time in various regions of the world as summarized by Pye et al. (2020) vs. known changes in NOx and SOx emissions in those regions.

Following the referee's suggestion, we looked at the historical record at Whiteface Mountain in New York and have added the following to the discussion of the buffering effect:

"The low sensitivity of cloudwater pH to strong acidity is seen in the long-term measurements of summertime cloudwater ions at Whiteface Mountain, NY (44°22'N, 73°54'W). Between 1994 and 2013, strong acidity at the site decreased by two-thirds, from about 300 to 100 µeq L^{-1}, but the VWA pH increased by only 0.8 units, from 3.8 to 4.6 (Schwab et al. 2016). At the same time, $[NH_4^+]$ decreased from about 125 to 60 µeq L^{-1} but collocated precipitation measurements showed no trend in NH_{3T} (Schwab et al. 2016). Carboxylate ions were not measured. These changes in cloudwater ion concentrations at Whiteface Mountain are similar to those in Fig. 5 and signify the pH buffering effect of NH_4^+ volatilization. Without this buffering, pH at the site would have increased by about 2.8 units."

7. The manuscript would benefit from a more detailed discussion of how cloud pH data were selected for comparison to model predictions. The authors include several observational studies in a number of regions, but certainly not all. I understand that some points are omitted due to source proximity and some, I think, were omitted due to being from an era far from the 2013 simulation and its emissions levels (although some fairly old measurements are included). Others (e.g., several studies from Japan mountain sites and the recent Kim et al. observations from the northern Pacific (https://doi.org/10.1007/s10874-020-09403-8)) are not included. A more robust discussion of why various datasets were included/excluded would give the reader greater confidence in the very promising matches shown with modeled pH values by region.

We have further clarified our criteria for selecting observations for comparison with the simulation. Page 7, lines 19-24 in the revised manuscript are as follows (underlined text added):
> …measured at mountain sites, coastal sites (marine fog), and from aircraft campaigns (Table A1). We exclude continental fogwater measurements because of their sensitivity to local emissions. The measurements span the period from 1980 to 2018, but we generally exclude observations made before 2005 in East Asia, Europe and the US because of the strong emission trends in these areas. We include some older measurements in the western US and northern Europe when there are no recent measurements in the particular region and the sites are relatively remote. Some of the observations are taken from the Pye et al. (2020) compilation."

Our compilation includes observations in Japan that were collected at Mt. Tateyama in 2007–09. All other cloudwater measurements in Japan that we are aware of were made before 2005 and thus were excluded from our compilation. We thank the referee for pointing out the observations by Kim et al. (2019) in the North Pacific. We had indeed missed them in our original compilation and now include them in the revised manuscript.

References
Collett, J. L., Hoag, K. J., Rao, X. and Pandis, S. N.: Internal acid buffering in San Joaquin Valley fog drops and its influence on aerosol processing, Atmos. Environ., 33(29), 4833–4847, doi:10.1016/S1352-2310(99)00221-6, 1999.

Kim, H. J., Lee, T., Park, T., Park, G., Collett, J. L., Park, K., Ahn, J. Y., Ban, J., Kang, S., Kim, K., Park, S.-M., Jho, E. H. and Choi, Y.: Ship-borne observations of sea fog and rain chemistry over the North and South Pacific Ocean, J. Atmos. Chem., 76(4), 315–326, doi:10.1007/s10874-020-09403-8, 2019.

Liljestrand, H. M.: Average rainwater pH, concepts of atmospheric acidity, and buffering in open systems, Atmospheric Environ. 1967, 19(3), 487–499, doi:10.1016/0004-6981(85)90169-6, 1985.

Schwab, J. J., Casson, P., Brandt, R., Husain, L., Dutkewicz, V., Wolfe, D., Demerjian, K. L., Civerolo, K. L., Rattigan, O. V., Felton, H. D. and Dukett, J. E.: Atmospheric Chemistry Measurements at Whiteface Mountain, NY: Cloud Water Chemistry, Precipitation Chemistry, and Particulate Matter, Aerosol Air Qual. Res., 16(3), 841–854, doi:10.4209/aaqr.2015.05.0344, 2016.

Stumm, Werner., Sigg, Laura. and Schnoor, J. L.: Aquatic chemistry of acid deposition, Environ. Sci. Technol., 21(1), 8–13, doi:10.1021/es00155a001, 1987.

Anonymous Referee #2
Received and published: 22 July 2020

Review of "Global modeling of cloudwater acidity, rainwater acidity, and acid inputs to ecosystems" by Shah et al.
This is a modeling study aiming to present a global view of cloud and rainwater pH, with particularly important aspects of the work including improved cloudwater pH calculations, inclusion of some carboxylic acids and dust alkalinity, and an explicit rainwater pH calculation. The topic is of relevance to the journal and addresses and important issue in the field of atmospheric sciences. I found the paper to be very well written, clear, and with conclusions well supported by the analysis. I recommend publication and do not have any additional suggestions for the authors.
We thank the referee for their comments.

Global modeling of cloudwater acidity, ~~rainwater~~precipitation acidity, and acid inputs to ecosystems

Viral Shah[1], Daniel J. Jacob[1,2], Jonathan M. Moch[2], Xuan Wang[1,a], Shixian Zhai[1]

[1]Harvard John A. Paulson School of Engineering and Applied Sciences, Harvard University, Cambridge, MA, USA.
[2]Department of Earth and Planetary Sciences, Harvard University, Cambridge, MA, USA.
[a] Now at School of Energy and Environment, City University of Hong Kong, Hong Kong SAR, China.

Correspondence to: Viral Shah (vshah@seas.harvard.edu)

Abstract. Cloudwater acidity affects the atmospheric chemistry of sulfate and organic aerosol formation, halogen radical cycling, and trace metal speciation. ~~Rainwater~~Precipitation acidity including post-depositional inputs adversely affects soil and freshwater ecosystems. Here we use the GEOS-Chem model of atmospheric chemistry to simulate the global distributions of cloud~~water~~ and ~~rainwater~~precipitation acidity, and the total acid inputs to ecosystems from wet deposition. The model accounts for strong acids (H_2SO_4, HNO_3, HCl), weak acids ($HCOOH$, CH_3COOH, CO_2, SO_2), and weak bases (NH_3, dust and sea salt aerosol alkalinity). We compile a global dataset of cloudwater pH measurements for comparison with the model. The global mean observed cloudwater pH is 5.2 ± 0.9, compared to 5.0 ± 0.8 in the model, with a range of 3 to 8 depending on region. The lowest values are over East Asia and the highest values are over deserts. Cloudwater pH over East Asia is low because of large acid inputs (H_2SO_4, HNO_3), despite NH_3 and dust neutralizing 70% of these inputs. Cloudwater pH is typically 4–5 over the US and Europe. Carboxylic acids account for less than 25% of cloudwater H^+ in the northern hemisphere on an annual basis, but 25–50% in the southern hemisphere and over 50% in the southern tropical continents where they push the cloudwater pH below 4.5. Anthropogenic emissions of SO_2 and NO_x (precursors of H_2SO_4 and HNO_3) are decreasing at northern mid-latitudes, but the effect on cloudwater pH is strongly buffered by NH_4^+ and carboxylic acids. The global mean ~~rainwater~~precipitation pH is 5.5 in GEOS-Chem, higher than the cloudwater pH because of dilution and below-cloud scavenging of NH_3 and dust. GEOS-Chem successfully reproduces the annual mean ~~rainwater~~precipitation pH observations in North America, Europe, and eastern Asia. Carboxylic acids, which are undetected in routine observations due to biodegradation, lower the annual mean ~~rainwater~~precipitation pH in these areas by 0.2 units. The acid wet deposition flux to terrestrial ecosystems taking into account the acidifying potential of NO_3^- and NH_4^+ in N-saturated ecosystems exceeds 50 meq m^{-2} a^{-1} in East Asia and the Americas, which would affect sensitive ecosystems. NH_4^+ is the dominant acidifying species in wet deposition, contributing 41% of the global acid flux to continents under N-saturated conditions.

1 Introduction

Cloudwater acidity (H^+ concentration) affects global atmospheric chemistry in a number of ways. It controls the rates of aqueous-phase reactions that (1) oxidize sulfur dioxide (SO_2) to sulfate aerosols (Martin et al., 1981; Calvert et al., 1985), (2)

oxidize dissolved organic compounds to less volatile forms leading to secondary organic aerosols (Ervens et al., 2011; Herrmann et al., 2015), and (3) convert halides into halogen radicals (von Glasow and Crutzen, 2003; Platt and Hönninger, 2003). It affects the solubility and bioavailability of iron in aerosol particles and thus the input of this micronutrient to marine ecosystems (Mahowald et al., 2005). Acidic deposition has a range of environmental effects on soil and freshwater ecosystems (Driscoll et al., 2001). Cloud~~water~~ and ~~rainwater~~precipitation acidity is affected in a complex way by natural and anthropogenic emissions, but there has been little effort so far to evaluate the ability of global models to represent this. Here we present such an evaluation with the GEOS-Chem atmospheric chemistry model and go on to discuss the factors controlling cloud~~water~~ and ~~rainwater~~precipitation acidity on a global scale.

Cloud~~water~~ and ~~rainwater~~precipitation H^+ concentrations are determined by the balance between dissolved acids (H^+ donors) and bases (H^+ acceptors). Sulfuric acid (H_2SO_4), nitric acid (HNO_3), and hydrogen chloride (HCl) are the major strong acids in the atmosphere, and they dissociate completely in cloud~~water~~ and ~~rainwater~~precipitation. The major weak acids are CO_2, SO_2, and carboxylic acids including formic acid ($HCOOH$)~~,~~ and acetic acid (CH_3COOH). Ammonia (NH_3) and alkaline dust particles are the major bases. Atmospheric acidity is commonly referenced to the CO_2–H_2O system (pH 5.6 at current CO_2 levels), with lower pH referred to as acidic conditions and higher pH as alkaline conditions. Cloudwater pH generally varies between 3 and 7, with highly acidic cloudwater typically found in industrialized areas with high SO_2 and nitrogen oxides (NO_x) emissions, and alkaline cloudwater found in agricultural and dusty areas (Warneck, 2000; Pye et al., 2020). ~~Rainwater~~Precipitation pH varies in a similar pattern (Dentener and Crutzen, 1994; Vet et al., 2014) but differs from cloudwater pH because of dilution (Weathers et al., 1988; Bormann et al., 1989), riming (Collett et al., 1993), below-cloud scavenging (Castillo et al., 1983; Zinder et al., 1988; Ayers and Gillett, 1988), and oxidation chemistry within raindrops (Overton et al., 1979; Graedel and Goldberg, 1983).

The chemical and physical processes governing cloud~~water~~ and ~~rainwater~~precipitation acidity have been well-established since the 1980s (Morgan, 1982; NRC, 1983; Stumm et al., 1987). They have been incorporated in many regional models focused on acid deposition (Chang et al., 1987; Venkatram et al., 1988; Carmichael et al., 1991; Hass et al., 1993; Olendrzynski et al., 2000; Langner et al., 2005) and global models focused on sulfur and nitrogen deposition (Dentener and Crutzen, 1994; Rodhe et al., 1995; Bouwman et al., 2002; Rodhe et al., 2002; Tost et al., 2007; Paulot et al., 2018). A few global modeling studies have focused on ~~rainwater~~precipitation pH (Dentener and Crutzen, 1994; Rodhe et al., 1995, 2002; Tost et al., 2007). These models calculated ~~rainwater~~precipitation [H^+] from the ~~rainwater~~precipitation concentrations of SO_4^{2-}, NO_3^-, NH_4^+, HCO_3^-, and CO_3^{2-} using ionic charge balance. Rodhe et al. (2002) also included dust alkalinity. None included carboxylic acids, which are known to be important but biodegrade rapidly after deposition (Keene et al., 1983; Keene and Galloway, 1984).

Cloudwater pH has received less attention in models. Some current global atmospheric chemistry models assume a constant cloudwater pH for aqueous reactions (S. Watanabe et al., 2011; Søvde et al., 2012), while others calculate it explicitly from

2

the balance of acids and bases but again generally neglecting dust alkalinity and carboxylic acids (Tost et al., 2007; Huijnen et al., 2010; Myriokefalitakis et al., 2011; Alexander et al., 2012; Lamarque et al., 2012; Simpson et al., 2012). Pye et al. (2020) presented the cloudwater pH values simulated by five such models and included a limited comparison with observations. They found large differences among models particularly in dusty areas where pH estimates varied by 3–4 units. All models showed large systematic biases compared to observations. In light of these findings, Pye et al. (2020) highlighted the need for improvements in the cloudwater simulations including further evaluation with observations.

Here we present a global analysis of cloudwater and rainwaterprecipitation pH in the GEOS-Chem model with an improved cloudwater pH calculation, including in particular carboxylic acids and dust alkalinity, and an explicit rainwaterprecipitation pH calculation. We evaluate the simulation with extensive cloudwater and rainwaterprecipitation measurements and determine the sources of acidity and alkalinity in different parts of the world. We examine the buffering effects of NH_3 and carboxylic acids on cloudwater pH, and the changes in acid inputs to terrestrial ecosystems from post-depositional processes.

2 Model description

We use the GEOS-Chem atmospheric chemistry model (www.geos-chem.org) version v11-02 with a number of modifications, some from more recent GEOS-Chem versions and some specifically from this work. The model is driven by assimilated meteorological fields from the NASA Global Modeling and Assimilation Office's Modern-Era Retrospective analysis for Research and Applications, version 2 (MERRA-2) system (Gelaro et al., 2017). These fields include in particular cloudwater liquid and ice content, cloud volume fraction, and 3-D liquid and ice precipitation fluxes, updated every three hours. GEOS-Chem includes detailed NO_x-hydrocarbon-aerosol-halogen chemistry (Mao et al., 2013; P. Kim et al., 2015; Travis et al., 2016; Sherwen et al., 2016), and here we have added recent halogen updates (X. Wang et al., 2019). The model distinguishes between fine and coarse aerosol but does not otherwise include aerosol microphysics. Wet deposition follows the algorithm of Liu et al. (2001) including rainout (in-cloud scavenging), washout (below-cloud scavenging), and scavenging in convective updrafts, with updates by Q. Wang et al. (2011) and Amos et al. (2012). Dry deposition follows a standard resistance-in-series scheme (Wesely, 1989; Y. Wang et al., 1998). We conduct the simulation on a global 4º latitude × 5º longitude grid for the year 2013 following an initialization period of one year.

2.1 Emissions and acid-producing chemistry

Here we describe the GEOS-Chem emissions and chemistry most relevant to the simulation of cloudwater and rainwaterprecipitation acidity. Emissions are calculated by the Harvard-NASA Emissions Component (HEMCO) (Keller et al., 2014). Default anthropogenic emissions of SO_2, NO_x, and NH_3 are from the global CEDS emissions inventory for 2013 (Hoesly et al., 2018). They are superseded by regional emissions inventories including MIX over Asia for 2010 (M. Li et al., 2017), MEIC over China for 2013 (Zheng et al., 2018), NEI 2011 over the US scaled to 2013 (Travis et al., 2016; U.S.

3

Environmental Protection Agency, 2018), APEI over Canada for 2013 (van Donkelaar et al., 2008), EMEP 2008 over Europe scaled to 2013 (EEA, 2019) and DICE over Africa for 2013 (Marais and Wiedinmyer, 2016). Ship SO_2 emissions are from Eyring et al. (2005). Ship NO_x emissions are from the ICOADS inventory (C. Wang et al., 2008) and are pre-processed with the PARANOX ship plume model (Vinken et al., 2011; Holmes et al., 2014). Aircraft emissions are from the AEIC inventory (Stettler et al., 2011). Biomass burning emissions are from GFED v4 (van der Werf et al., 2017). Natural emissions include NO_x from lightning (Murray et al., 2012) and soil (Hudman et al., 2012), volcanic SO_2 (Fisher et al., 2011), marine dimethyl sulfide (DMS) (Breider et al., 2017), and NH_3 from oceans, natural soils, and human population (Bouwman et al., 1997). Sea salt aerosol emissions in two size classes (fine and coarse) follow Jaeglé et al. (2011). Dust emissions include desert and semi-desert sources (Fairlie et al., 2007; Ridley et al., 2013), and combustion and industrial sources (Philip et al., 2017) in four size classes (one fine and three coarse). Biogenic volatile organic compounds (VOC) emissions are from MEGAN (Guenther et al., 2012; Hu et al., 2015).

Sulfur chemistry in GEOS-Chem includes oxidation of DMS to SO_2 and methanesulfonic acid (MSA), gas-phase oxidation of SO_2 to H_2SO_4, and aqueous-phase oxidation of SO_2 to H_2SO_4 in clouds, rain, and alkaline sea salt aerosols (Alexander et al., 2005, 2009; Q. Chen et al., 2017). Nitrogen chemistry includes oxidation of NO_x to HNO_3 in the gas phase, and in the aqueous phase of aerosols and clouds (McDuffie et al., 2018; Holmes et al., 2019). Tropospheric HCl is mainly from acid displacement reactions on sea salt aerosols (X. Wang et al., 2019).

HNO_3, HCl, and NH_3 are semi-volatile and their gas-particle partitioning affects their scavenging efficiency in cloudwater and rainwaterprecipitation (Amos et al., 2012). We calculate this partitioning at bulk thermodynamic equilibrium using ISORROPIA II for the H_2SO_4-HNO_3-HCl-NH_3-NVC metastable aqueous system, where NVC represents the non-volatile cations from fine-mode sea salt aerosol (X. Wang et al., 2019). The uptake of HNO_3 and release of HCl (acid displacement) on coarse-mode sea salt aerosol is treated as a kinetic process (X. Wang et al., 2019).

2.2 Simulation of HCOOH and CH₃COOH

The most important carboxylic acids for cloudwater and rainwaterprecipitation acidity are HCOOH (pK_a = 3.8 at 298K) and CH_3COOH (pK_a = 4.8 at 298K) (Morgan, 1982; Keene et al., 1983). They are present in the atmosphere at comparable concentrations (Talbot et al., 1997) but HCOOH is more important for contributing to acidity because of its higher Henry's law solubility and lower pK_a. Sources of these acids include secondary production from VOC oxidation and direct emissions from biomass burning, fossil-fuels, soils, and vegetation (Khare et al., 1999), but these are poorly understood and models greatly underestimate atmospheric concentrations (Paulot et al., 2011; Stavrakou et al., 2012; Millet et al., 2015; Khan et al., 2018). Here we use the previous GEOS-Chem HCOOH simulation by Millet et al. (2015) which scales up the biogenic emissions from the MEGAN inventory (Guenther et al., 2012) in order to fit atmospheric observations over the US. This yields a global HCOOH source of 1900 Gmol a^{-1}. Stavrakou et al. (2012) previously estimated a global HCOOH source of 2200–

2600 Gmol a^{-1} from inversion of satellite data. In addition, we assume a minimum background mixing ratio of 100 pptv (50 pptv south of 60°S), based on measurements in the marine boundary layer and the free troposphere (Arlander et al., 1990; Talbot et al., 1990, 1997; Legrand et al., 2004) and satellite-derived free troposphere HCOOH columns over marine areas of 1–2×10^{15} molecules cm^{-2} (Franco et al., 2020).

5

Our CH$_3$COOH simulation follows the standard GEOS-Chem mechanism (Mao et al., 2013; Travis et al., 2016) without further improvement, except that the minimum background CH$_3$COOH concentration is also taken to be 100 pptv (50 pptv south of 60°S), based on observations in the marine boundary layer and the free troposphere (Arlander et al., 1990; Talbot et al., 1990, 1997; Helas et al., 1992; Franco et al., 2020). The global simulated CH$_3$COOH source is 1000 Gmol a^{-1}. Other modeling studies

10   attempting to fit CH$_3$COOH observations have estimated a source in the range 1700–3900 Gmol a^{-1} (Baboukas et al., 2000; Khan et al., 2018).

Figure 1 compares annual mean GEOS-Chem wet deposition fluxes of HCOOH and CH$_3$COOH with observations from the compilations of Vet et al. (2014) and Keene et al. (2015). We find that the mean GEOS-Chem HCOOH flux (7.5 mmol m^{-2}

15   a^{-1}) is consistent with the mean of the observations (6.9 mmol m^{-2} a^{-1}). The model captures the high fluxes observed in the tropical continents where there are large biogenic sources, and the low fluxes observed at marine sites. GEOS-Chem underestimates the CH$_3$COOH flux by a factor of 4. The observed patterns of HCOOH and CH$_3$COOH fluxes are similar, suggesting that model CH$_3$COOH could be corrected similarly to HCOOH in future work by scaling up biogenic emission. But the effect is relatively small. We find in the model that the global mean cloudwater pH would decrease by 0.05 units if we

20   increased CH$_3$COOH concentrations by a factor of 4.

2.3 Calculation of cloudwater and ~~rainwater~~precipitation composition and pH

Cloudwater composition is computed locally in each grid cell containing liquid cloudwater over 30-min time steps using the in-cloud liquid water content and cloud volume fraction from MERRA-2. Dissolution of gases in the cloud droplets follows the Henry's law constants of Table 1 and acid/base dissociation constants of Table 2. We assume that 70% of fine aerosol mass

25   and 100% of coarse aerosol mass are partitioned into cloudwater (Hegg et al., 1984; Alexander et al., 2012). Sulfate-nitrate-ammonium and sea salt particles dissolve completely in cloudwater, and the alkaline component of the dust particles also dissolves. Freshly emitted sea salt particles contain an alkalinity of 0.07 eq kg^{-1} (Alexander et al., 2005), while freshly emitted dust particles contain an alkalinity of 4.5 eq kg^{-1} based on the assumption of 7.1% Ca^{2+} and 1.1% Mg^{2+} by dry mass (Engelbrecht et al., 2016) with CO$_3^{2-}$ as anion. Sea salt NVCs are expressed as Na$^+$ equivalents, while dust NVCs are expressed

30   as Ca^{2+} equivalents. The upper limit of Ca^{2+} concentration is set by formation of CaCO$_3$(s).

The calculation of cloudwater composition in the cloudy fraction of each grid cell assumes a closed system where the summed concentrations of gas and cloudwater species in Table 3 are conserved, and the partitioning is then computed following the

5

equilibria of Tables 1 and 2. The calculation is done by solving the electroneutrality equation iteratively using Newton's method (Moch et al., 2020). This improves on the original calculation of cloudwater composition in GEOS-Chem (Alexander et al., 2012) through the inclusion of additional acidic and alkaline species (HCl, HCOOH, CH₃COOH, NVCs) and using a more stable numerical solver.

5

We will present results as time averages (mainly annual) and spatial averages (vertical or zonal). The time- and space- averaged cloudwater [H⁺] cannot be calculated directly from the [H⁺] computed at each model time step in each grid cell because [H⁺] is a non-conservative quantity controlled by the other acidic and basic species in cloudwater (Liljestrand, 1985). Therefore, we calculate the average cloudwater [H⁺] from the corresponding volume weighted average (VWA) concentrations of the cloudwater ions. We assume that all acids and bases except carbonates are conserved in the aqueous phase. For HCOOH and CH₃COOH, the total (dissociated + undissociated) amounts are assumed to be conserved. Thus, the time- and space-averaged cloudwater [H⁺] is given by:

$$\overline{[\text{H}^+]} = 2\overline{[\text{SO}_4^{2-}]} + \overline{[\text{NO}_3^-]} + \overline{[\text{Cl}^-]} + \overline{[\text{HSO}_3^-]} + 2\overline{[\text{SO}_3^{2-}]} + \overline{[\text{HCOO}^-]} + \overline{[\text{CH}_3\text{COO}^-]} + \overline{[\text{HCO}_3^-]} - \overline{[\text{NH}_4^+]} - 2\overline{[\text{Ca}^{2+}]} - \overline{[\text{Na}^+]} \quad (1)$$

where $\overline{[\text{A}]}$ represents the VWA molar concentration in cloudwater of species A over the time period and spatial domain of interest. We calculate $\overline{[\text{A}]}$ from the concentration of the species, $[\text{A}]_{i,j}$, and the cloud liquid water content, $L_{i,j}$, at each model time step i and grid cell j:

$$\overline{[\text{A}]} = \frac{\sum_{j=1}^{m}\sum_{i=1}^{t} L_{i,j}\,[\text{A}]_{i,j}}{\sum_{j=1}^{m}\sum_{i=1}^{t} L_{i,j}} \quad (2)$$

where $[1, t]$ is the averaging time period and $[1, m]$ is the ensemble of grid cells included in the average. $\overline{[\text{CO}_3^{2-}]}$ and $\overline{[\text{OH}^-]}$ are negligible compared to other anions over the range of cloudwater pH values (< 8). $\overline{[\text{HCOO}^-]}$ is calculated from the total aqueous concentration, $\overline{[\text{HCOOH}]_{aq,T}} = \overline{[\text{HCOOH}]_{aq}} + \overline{[\text{HCOO}^-]}$, as follows:

$$\overline{[\text{HCOO}^-]} = \left(\frac{K_a}{K_a + \overline{[\text{H}^+]}}\right)\overline{[\text{HCOOH}]_{aq,T}} \quad (3)$$

where K_a is the HCOOH(aq)/HCOO⁻ acid dissociation constant from Table 2 computed at the average cloudwater temperature for the time period and spatial domain. The same procedure is used for $\overline{[\text{CH}_3\text{COO}^-]}$. $\overline{[\text{HCO}_3^-]}$ is calculated from equilibrium with atmospheric CO₂ as follows:

$$\overline{[\text{HCO}_3^-]} = \frac{H_{\text{CO}_2} K_{c1} P_{\text{CO}_2}}{\overline{[\text{H}^+]}} \quad (4)$$

where H_{CO_2} and K_{c1} are the Henry's law coefficient for CO₂ and the CO₂(aq)/HCO₃⁻ acid dissociation constant, respectively, at the average cloudwater temperature for the period and domain (Tables 1 and 2). P_{CO_2} is the CO₂ partial pressure, taken to be 390 ppm as representative of 2013. Substituting these values in Eq. (4), $\overline{[\text{HCO}_3^-]} \approx 10^{-11.3}/\overline{[\text{H}^+]}$. Over the range of cloudwater pH values (3–8.5), $\overline{[\text{CO}_3^{2-}]}\left(\approx 10^{-21.6}/\overline{[\text{H}^+]}^2\right)$ and $\overline{[\text{OH}^-]}\left(\approx 10^{-14}/\overline{[\text{H}^+]}\right)$ are negligible compared to $\overline{[\text{HCO}_3^-]}$

6

and omitted from Eq. (1) (Stumm et al., 1987). Since $\overline{[HCOO^-]}$, $\overline{[CH_3COO^-]}$, and $\overline{[HCO_3^-]}$ calculated in this way depend on $\overline{[H^+]}$, Eq. (1) is cubic in $\overline{[H^+]}$. The time- and space-averaged pH ($\overline{pH}$) is calculated from $\overline{[H^+]}$:

$$\overline{pH} = -\log_{10}\left(\overline{[H^+]}\right) \tag{5}$$

5   There is some arbitrariness in assuming that NH_3, SO_2, and carboxylic acids do not equilibrate with the gas phase during averaging. We examined the sensitivity to this assumption by assuming alternatively that NH_{3T}, SO_{2T}, $HCOOH_T$ and CH_3COOH_T as defined in Table 3 (sum of gas-phase and aqueous-phase concentrations) are conserved and recalculating the gas–cloudwater equilibrium for the time-averaged conditions. We find no significant difference in the computed $\overline{[H^+]}$.

10   Calculation of ~~rainwater~~precipitation VWA composition including $\overline{[H^+]}$ follows the same approach as for cloudwater. In that case we use the model-archived wet deposition fluxes including contributions from in-cloud and below-cloud scavenging. We assume that SO_2 is instantly oxidized by H_2O_2 (as available) in ~~rainwater~~precipitation and is scavenged as SO_4^{2-}. As with cloudwater, the maximum $[Ca^{2+}]$ is set by the formation of $CaCO_3(s)$. ~~Rainwater~~Precipitation pH measurements are generally reported as monthly means and do not account for HCOOH and CH_3COOH, which biodegrade rapidly. To compare with

15   measurements, we calculate a monthly $\overline{[H^+]}$ for each grid cell by removing $\overline{[HCOO^-]}$ and $\overline{[CH_3COO^-]}$ from the charge balance in Eq. (1). From there we calculate the annual precipitation VWA pH:

$$\overline{pH_{VW}} = -\log_{10}\left(\frac{\sum_{k=1}^{12} P_k \overline{[H^+]}_k}{\sum_{k=1}^{12} P_k}\right) \tag{6}$$

where $\overline{[H^+]}_k$ is the mean ~~rainwater~~precipitation $[H^+]$ and P_k is the precipitation depth for month k.

3 Results and discussion

20   **3.1 Global distribution of cloudwater pH and composition**

    Figure 2 shows the global distribution of cloudwater pH as simulated by GEOS-Chem and as measured at mountain sites, coastal sites (marine fog), and from aircraft campaigns (Table A1). We exclude continental fogwater measurements because of their sensitivity to local emissions. The measurements span the period from 1980 to 2018, but we generally exclude observations made before 2005 in East Asia, Europe and the US because of the strong emission trends in these areas. ~~but near~~

25   ~~source regions we only include observations made after 2006.~~ We include some older measurements in the western US and northern Europe when there are no recent measurements in a particular region and the sites are relatively remote. Some of the observations are taken from the Pye et al. (2020) compilation.

    The top panel shows the mean observed and simulated pH values. The observed values are as reported in the literature, where

30   the computation of the mean is generally based on VWA $[H^+]$. The model values are annual means below 700 hPa ($\approx$3 km

above sea level) for the year 2013. The bottom panel shows the observations aggregated by regions and arranged in ascending pH order, along with the corresponding GEOS-Chem values. For comparison with the observations, the model is sampled at the locations and months of the measurements.

5   The global mean cloudwater pH in the observations is 5.2 ± 0.9, compared to 5.0 ± 0.8 in the model. Annual mean values in Fig. 2 range from 3 to 8, showing distinct spatial patterns. The spatial patterns can be understood from the distributions of acidic and basic ions shown in Fig. 3. Na^+ and Cl^- are major constituents of cloudwater in marine and coastal areas but are not shown in the Fig. 3 because they are largely in balance and have little net effect on pH. Figure 3 also shows the percent contribution of each ion to the total anion or cation concentrations (contour lines).

10

The lowest pH values are generally over East Asia, both in the observations and in the model, with values mostly below 4.3 in eastern and /southern China and Japan. This is due in GEOS-Chem to extremely high $[SO_4^{2-}]$ and $[NO_3^-]$, and despite 70% of these anions being balanced by NH_4^+ and dust cations. pH values remain low over the North Pacific (~4.5), despite much lower acid inputs, because less than half of the acidic anions are balanced by bases.

15

Over the US and Europe, average pH values are in the range 4–5 both in the observations and in the model, with most of the acidity as NO_3^-, and NH_4^+ balancing over 50% of the acidic anions. The model shows higher values in the central US (~5.5) because of NH_3 and dust emissions. Summertime observations in the southwest US by Hutchings et al. (2009) show a pH of 6.3 due to large dust influence, but this seasonal dust emission is underestimated in GEOS-Chem (Fairlie et al., 2007). Over
20   southern Europe, about 25% of the base cations are from Saharan dust. NH_4^+ is the main cation elsewhere in Europe. SO_4^{2-} is the dominant acidic component over the northern midlatitude oceans because of the oceanic source of SO_4^{2-} from the oxidation of DMS and because continental influence extends further for SO_4^{2-} than for NO_3^- (Heald et al., 2006). Over the Arctic, the simulated pH is much lower (4–4.5) because of long-range transport of acidic species and less than 50% neutralization (Fisher et al., 2011).

25

The carboxylate ions $HCOO^-$ and CH_3COO^- account for less than 25% of H^+ throughout the extratropical northern hemisphere (Fig. 3). The carboxylic acids are more important relative contributors to H^+ in the tropics and in the southern hemisphere, exceeding 50% in some areas of the tropical continents and southern midlatitudes. Ayers and Gillett (1988) found that carboxylic acids were responsible for observed cloudwater pH below 4 over tropical Australia, but GEOS-Chem
30   underestimates carboxylic acids in that region (Fig. 1). Carboxylates were not measured in the Ecuador cloudwater measurements (Makowski Giannoni et al., 2016), but we find from the model that the carboxylic acids contribute about 50% of the H^+. GEOS-Chem shows similar pH values as observed at Cape Grim (mean of 5.5), reflecting the low concentrations of acidic and basic species from continental sources. Cloudwater pH sampled on the Antarctic coast also has a mean pH of 5.5

(Saxena and Lin, 1990) but the model is much lower over the Antarctic coast because of SO_4^{2-} from oxidation of DMS. This may be because of sea salt alkalinity from blowing snow that is not accounted for in the model (Huang et al., 2018).

Alkaline cloudwater (pH > 5.6) is found in the observations over western India, Tibet, and Morocco, consistent with the model where the alkalinity is mainly from dust. GEOS-Chem simulates pH of 6–8 over the area extending from the Sahara to the Gobi Desert. The transport of dust alkalinity from North Africa raises the cloudwater pH in the Caribbean to above 5.5, both in the observations (Gioda et al., 2011) and in the model.

Figure 4 shows the zonal mean distributions of cloudwater pH and cloud liquid water content (contour lines). In addition to the latitudinal variations described previously, cloudwater pH increases as the cloud liquid water content increases because of the effect of dilution. Liquid water content peaks at about 900 hPa, and decreases at higher altitudes, and this largely explains the mean variation of pH with altitude.

Pye et al. (2020) showed in their review the annual mean tropospheric-column cloudwater pH from three models: CMAQ (northern hemisphere only), TM4-ECPL, and GEOS-Chem. They calculated the annual mean pH using VWA [H^+] rather than Eq. (1). We find that their calculation method underestimates the pH over alkaline regions by 1–3 units but has little error for acidic regions. The GEOS-Chem results shown in Pye et al. (2020) follow the previous cloudwater [H^+] calculation from Alexander et al. (2012), which is different from our calculation (Sect. 2). The resulting pH values are comparable over industrialized regions but differ by up to 2 units over tropical forests and deserts because carboxylic acids and dust alkalinity were not ~~previously~~ included. ~~pH values were~~They are also generally higher than 6 over the oceans ~~in the previous GEOS-Chem simulation~~ because of an error in the numerical solver. The pH values shown by Pye et al. (2020) for TM4-ECPL are lower than our simulation by 1–2 units over most areas, and would be inconsistent with the observations shown in Fig. 2. Our pH estimates are closest to those from CMAQ, which was the only model in Pye et al. (2020) that included dust alkalinity and HCOOH in the cloud water pH calculation. The zonal mean cloud water pH values from the ECHAM5/MESSy1 model presented by Tost et al. (2007) are 0.2–0.3 units higher than our values, likely because of their omission of carboxylic acids.

Emissions of SO_2 and NO_x in the northern mid-latitude continents are decreasing rapidly because of air quality concerns (Hoesly et al., 2018; Zheng et al., 2018). Considering that NH_3 and dust neutralize presently balance over 50% of the acidic anions over these continents (Fig. 3), one might expect large increases in cloudwater pH as SO_2 and NO_x emissions decrease. There is however a large buffering effect from the semi-volatile carboxylic acids and NH_3. Consider the case of the US. Figure 5 shows the mean simulated cloudwater composition for 2013 over the continental US, and the change in composition resulting from a factor of two decrease in strong acidity (SO_4^{2-} +, NO_3^-). The total concentrations of carboxylic acids ($RCOOH_T \equiv HCOOH_T + CH_3COOH_T$) and ammonia ($NH_{3T}$) are held at 2013 levels and the gas–cloudwater equilibrium is recalculated. For 2013, the mean cloudwater pH is 4.7, a level at which only one-fourth of $RCOOH_T$ is present as carboxylate ions, and most of

the NH$_{3T}$ is present as NH$_4^+$. Decreasing the strong acidity by half triples the dissociated fraction of RCOOH$_T$ and volatilizes a significant fraction of NH$_4^+$, which limits the increase in cloudwater pH to 5.7. Without this buffering effect, the pH would have increased by 2.1 units to 6.8. NH$_4^+$ volatilization exerts a stronger buffering effect than carboxylic acid dissolution because NH$_{3T}$ concentrations are much larger. Buffering by CO$_2$ and SO$_2$ becomes important at pH values above 6 (Liljestrand, 1985) and buffering by higher organic acids is important in highly polluted areas (Collett et al., 1999).

The low sensitivity of cloudwater pH to strong acidity is seen in the long-term measurements of summertime cloudwater ions at Whiteface Mountain, NY (44°22'N, 73°54'W). Between 1994 and 2013, strong acidity at the site decreased by two-thirds, from about 300 to 100 µeq L^{-1}, but the VWA pH increased by only 0.8 units, from 3.8 to 4.6 (Schwab et al. 2016). At the same time, [NH$_4^+$] decreased from about 125 to 60 µeq L^{-1} but collocated precipitation measurements showed no trend in NH$_{3T}$ (Schwab et al. 2016). Carboxylate ions were not measured. These changes in cloudwater ion concentrations at Whiteface Mountain are similar to those in Fig. 5 and signify the pH buffering effect of NH$_4^+$ volatilization. Without this buffering, pH at the site would have increased by about 2.8 units.

3.2 Global distribution of ~~rainwater~~precipitation pH and composition

Figure 6 (left panel) shows the global distribution of annual mean ~~rainwater~~precipitation pH for the year 2013. ~~Here we define 'rainwater' as all precipitation water (both rain and snow).~~ The pH averaging procedure is as described in Sect. 2.3. The global mean ~~rainwater~~precipitation $\overline{\text{pH}}$ is 5.5 and varies from 4.5 over industrialized areas and the tropical forests to 8 over deserts, showing the same spatial patterns as cloudwater pH but with lower acidity because of dilution. Figure 7 shows the simulated concentrations of ~~rainwater~~precipitation ions, except for Na$^+$ and Cl$^-$ which again do not contribute significantly to net acidity. ~~Rainwater~~Precipitation ion concentrations are on average 4 times more dilute than cloudwater concentrations (Fig. 3). The relative contribution of SO$_4^{2-}$ in industrialized regions is higher than for cloudwater because of additional SO$_4^{2-}$ from below-cloud scavenging of SO$_2$. The NO$_3^-$ contribution in central Africa is higher than for cloudwater because of high-altitude convective scavenging of HNO$_3$ produced from lightning NO$_x$. In Amazonia and tropical Africa, HCOO$^-$ and CH$_3$COO$^-$ contribute a larger fraction of ~~rainwater~~precipitation acidity compared to cloudwater because of below-cloud scavenging, and as a result the ~~rainwater~~precipitation pH is similar to that of cloudwater. Similarly, below-cloud scavenging of desert-generated dust results in alkaline ~~rainwater~~precipitation over a much larger area compared to cloudwater.

The right panel in Fig. 6 shows the change in ~~rainwater~~precipitation pH when the contribution from carboxylic acids is excluded. These acids biodegrade quickly, and thus their acidity is not generally captured by ~~rainwater~~precipitation pH measurements. We find that ~~rainwater~~precipitation pH increases by 0.4–1 unit in the Amazon, tropical Africa, and southeast Asia, consistent with observations (Andreae et al., 1990; Sanhueza et al., 1992; Sigha-Nkamdjou et al., 2003; Yoboué et al., 2005). Over the US, Europe, and eastern China the increase in pH is 0.1–0.4 units, which is similar to the observed contribution of carboxylic acids to ~~rainwater~~precipitation H$^+$ (10–60%) in these areas (Keene and Galloway, 1984; Kawamura et al., 1996;

10

Peña et al., 2002; Xu et al., 2010; Niu et al., 2018). Over the oceans, the change in pH from HCOOH and CH₃COOH is small (~0.15 units) and in agreement with marine observations (Keene et al., 2015).

Figure 8 compares the simulated annual VWA ~~rainwater~~precipitation pH ($\overline{pH_{VW}}$, Eq. 6) with observations from monitoring networks for the year 2013. Precipitation (rain and snow) pH observations are from the US National Trends Network (NTN) (NADP, 2019), the Canadian Air and Precipitation Monitoring Network (CAPMoN) (ECCC, 2018) , the European Monitoring and Evaluation Programme (EMEP) (EMEP, 2015), and the Acid Deposition Monitoring Network in East Asia (EANET) (EANET, 2019). We use monthly mean measurements from NTN (249 sites), EMEP (83 sites), and EANET (45 sites) and daily measurements from CAPMoN (30 sites), which we average to a monthly VWA [H⁺]. The monthly [H⁺] values are used to calculate $\overline{pH_{VW}}$ following Eq. (6). The acidity from HCOO⁻ and CH₃COO⁻ is not accounted in the network measurements unless treated with biocide, which is done only in Malaysia. Thus, for comparison with observations, we use the simulated $\overline{pH_{VW}}$ calculated without HCOO⁻ and CH₃COO⁻.

GEOS-Chem ~~rainwater~~precipitation pH values are largely consistent with the observations, reproducing the observed regional means to within 0.1 pH unit (observed: 5.26–5.30, GEOS-Chem: 5.23–5.39). Carboxylic acids lower the mean GEOS-Chem pH by 0.15–0.2 units. The model also generally reproduces the observed spatial variations within the regions. Observations and model show higher pH in the Midwest than in the rest of the US because of neutralization by agricultural NH₃. ~~Rainwater~~Precipitation pH in southern Europe is also relatively high because of Saharan dust influence. Model values there are lower than in Fig. 6 because of different forms used to calculate annual mean pH (Eq. 6 here instead of Eq. 1). High [SO₄²⁻] and [NO₃⁻] ~~and moderate neutralization~~ lower the ~~rainwater~~precipitation pH to below 4.5 in eastern China, Korea, and Japan. The high pH value observed in Xi'an (central China) is due to alkalinity from dust sources (EANET, 2016) but the corresponding dust influence in the model is shifted slightly to the northwest. The low pH observed over Chongqing (central China) is because of high SO₂ and NOₓ emissions which are trapped locally by the surrounding terrain (Y. Chen et al., 2017).

Our global distribution of ~~rainwater~~precipitation pH can be compared to previous model simulations by Rodhe et al. (2002) and Tost et al. (2007). Neither included carboxylic acids and thus they overestimated pH values over tropical continents. Tost et al. (2007) did not include dust alkalinity either, resulting in large pH underestimates over desert regions. The pH values over eastern North America and Europe in these previous studies are about 0.5 units lower than in our simulation, reflecting the more recent decreases in SO₂ and NOₓ emissions (Hoesly et al., 2018).

3.3 Soil and freshwater acidification by wet deposition

Acidification of soil and freshwater is one of the major adverse effects of wet deposition fluxes on ecosystems because it causes the leaching of nutrients, mobilizes toxic metals, and directly damages biota (Driscoll et al., 2001). Quantifying this effect requires accounting for post-depositional processes. The H⁺ flux associated with carboxylates and HCO₃⁻ is not relevant

11

because carboxylic acids are readily consumed by bacteria, and the amount of HCO_3^- in ecosystems is controlled by the ambient CO_2 concentrations (Reuss and Johnson, 1986). The acidifying effects of NO_3^- and NH_4^+ depend on the biotic demand for nitrogen (N) (Reuss and Johnson, 1986). In ecosystems with high N demand (so-called N-limited ecosystems), NO_3^- and NH_4^+ are readily assimilated by plants and microbes. Uptake of NO_3^- is accompanied by the uptake of H^+ (or release of OH^-), cancelling the acidic effect of NO_3^- deposition. NH_4^+ uptake is accompanied by the release of H^+, reversing the neutralizing effect of NH_4^+. Therefore, in N-limited ecosystems the acidic flux is calculated as follows (Rodhe et al., 2002):

$$F_{H^+(N\text{-}lim)} = F_{SO_4^{2-}} - F_{dust\ NVC} \tag{7}$$

where F denotes the wet deposition flux in equivalents. However, in many industrialized regions, N deposition greatly exceeds the biotic demand and results in N-saturated conditions (Aber et al., 1989; Watmough et al., 2005; Gundersen et al., 2006; Duan et al., 2016). In such conditions, only a small fraction of the deposited NO_3^- and NH_4^+ is assimilated. The excess NO_3^- causes H^+ accumulation, while the excess NH_4^+ can be converted by microbes to NO_3^- (nitrification), which releases $2H^+$ for every NH_4^+ converted and also results in net H^+ formation. Considering the full acidifying potential of NO_3^- and NH_4^+, we calculate the acidic flux in N-saturated conditions as follows (Galloway, 1995; Rodhe et al., 2002):

$$F_{H^+(N\text{-}sat)} = F_{SO_4^{2-}} + F_{NO_3^-} + F_{NH_4^+} - F_{dust\ NVC} \tag{8}$$

$F_{H^+(N\text{-}sat)}$ can be viewed as the upper limit of acidic inputs through wet deposition as some of the accumulated NO_3^- can denitrify to N_2.

Figure 9 shows $F_{H^+(N\text{-}lim)}$ and $F_{H^+(N\text{-}sat)}$, along with the free H^+ flux which represents the direct acid input to ecosystems excluding carboxylic acids. The global mean $F_{H^+(N\text{-}lim)}$ over continents (4.1 meq m^{-2} a^{-1}) is higher than the mean free H^+ flux (3.1 meq m^{-2} a^{-1}). The free H^+ flux is higher than $F_{H^+(N\text{-}lim)}$ over central Africa and Amazonia because of H^+ associated with NO_3^- and HCO_3^-, respectively. $F_{H^+(N\text{-}lim)}$ is highest over the eastern US, Central and South America, and East Asia, reflecting high SO_4^{2-} fluxes. The global mean $F_{H^+(N\text{-}sat)}$ over continents (18 meq m^{-2} a^{-1}) is much larger than $F_{H^+(N\text{-}lim)}$ and the free H^+ flux because of acidity generated from NH_4^+ nitrification. Over eastern India, East and Southeast Asia, the eastern US, and Central and South America, $F_{H^+(N\text{-}sat)}$ is more than 50 meq m^{-2} a^{-1}, which exceeds the critical load for acidification of highly sensitive ecosystems with low acid buffering capacity (Kuylenstierna et al., 2001; Bouwman et al., 2002).

The total wet deposition of individual ions over the continents is largest for NH_4^+ (1.3×10^{12} eq a^{-1}) followed by SO_4^{2-} (1.0×10^{12} eq a^{-1}) and NO_3^- (0.85×10^{12} eq a^{-1}). Lamarque et al. (2013) reported that for the year 2000 the multi-model mean ($\pm$ standard deviation) of the wet deposition flux over continents was higher for SO_4^{2-} ($1.5 \pm 0.3 \times 10^{12}$ eq a^{-1}) than for NH_4^+ ($1.2 \pm 0.3 \times 10^{12}$ eq a^{-1}) and NO_3^- ($1.1 \pm 0.2 \times 10^{12}$ eq a^{-1}). The decrease in the SO_4^{2-} wet deposition flux between 2000 and 2013 reflects the global decrease of anthropogenic SO_2 emissions (Hoesly et al., 2018). We find that NH_4^+ is now the largest source of

acidifying wet deposition, contributing 41% of $F_{H^+(N\text{-}sat)}$ over continents globally, and it will contribute even more in the future as global NH₃ emissions continue to grow (Hoesly et al., 2018).

4 Conclusions

We used the GEOS-Chem global model of atmospheric chemistry to simulate the global distributions of cloudwater and ~~rainwater~~precipitation acidity, and the total acid inputs from wet deposition to terrestrial ecosystems. This involved an improved pH calculation in GEOS-Chem including contributions from dust alkalinity, sea salt aerosol alkalinity, and carboxylic acids (HCOOH and CH₃COOH). Our prime motivation was to better understand and evaluate the global cloudwater pH distribution in the model for future simulations of sulfate, organic, and halogen chemistry. Extending the analysis to ~~rainwater~~precipitation pH provided further opportunity for model evaluation and allowed us to quantify post-depositional effects in acid inputs to ecosystems on a global scale.

We compiled cloudwater pH measurements worldwide from the literature and compared them to the GEOS-Chem simulation. The global mean cloudwater pH is 5.2 ± 0.9 in the observations, and 5.0 ± 0.8 in GEOS-Chem sampled at the same locations. The lowest pH values of 3–4 are over East Asia because of high acid inputs and despite an average 70% neutralization by NH₃ and dust cations. Low pH values extend across the North Pacific because of weak neutralization. Cloudwater pH is 4–5 over the US and Europe with dominant acid input from HNO₃ and over 50% neutralization from NH₃. Alkaline cloudwater with pH as high as 8 is found over the northern subtropical desert belt extending from the Atlantic Ocean to Mongolia, including western India. Carboxylic acids account for less than 25% of the cloudwater H⁺ in the northern hemisphere, but 25–50% in the southern hemisphere and over 50% in the southern tropical continents where they drive the pH to below 4.5. We find little dependence of cloudwater pH on altitude other than dilution from changes in liquid water content.

Anthropogenic emissions of SO₂ and NOₓ are decreasing rapidly in the developed world, and this together with the large fraction of neutralized acidity might be expected to lead to large increases in cloudwater pH. However, there is a strong buffering effect because of the semi-volatility of NH₄⁺ and carboxylates. We find that a factor of 2 decrease in SO₄²⁻ and NO₃⁻ inputs over the US increases the cloudwater pH by 1 unit, compared to an increase of 2.1 units in the absence of buffering.

The global mean ~~rainwater~~precipitation pH in GEOS-Chem is 5.5, higher than cloudwater pH because of dilution and below-cloud scavenging of bases (NH₃, dust). ~~Rainwater~~Precipitation pH shows spatial patterns similar to cloudwater pH but is influenced more strongly by carboxylic acids and dust near source regions because of below-cloud scavenging. GEOS-Chem is consistent with the annual mean ~~rainwater~~precipitation pH observed at monitoring networks in North America, Europe, and East Asia. We find that the carboxylic acids lower the ~~rainwater~~precipitation pH by up to 1 unit in the Amazon, tropical Africa,

and southeast Asia, and by about 0.2 units in the US, Europe, and East Asia. This pH depression would not be seen in the observations because of fast biological consumption of the carboxylic acids after deposition.

Carboxylic acids affect cloudwater and precipitation pH globally, but their sources are uncertain. Our simulation could reproduce the observed HCOOH wet deposition flux by using scaled-up biogenic emissions but underestimated CH_3COOH flux by a factor of 4, indicating that a better understanding of their sources is needed. Dicarboxylic acids, such as oxalic, succinic, and malonic acids, are also present in cloudwater and precipitation and their effect on pH needs to be evaluated.

Lastly, we examined the total acid inputs to soil and freshwater from wet deposition, including the post-depositional effects from NH_4^+ and NO_3^- utilization by the biosphere. We find that total acid inputs under N-saturated conditions exceed 50 meq m^{-2} a^{-1} in many parts of East Asia and the Americas, a level that can damage sensitive ecosystems. NH_4^+ contributes 41% of the acid input under N-saturated conditions globally.

Author contributions: VS and DJJ designed the study. VS carried out the modeling and analysis. JMM, XW, and SZ contributed model updates. VS and DJJ wrote the paper with input from all authors.

Competing interests: The authors declare that they have no conflict of interest.

References

Aber, J. D., Nadelhoffer, K. J., Steudler, P. and Melillo, J. M.: Nitrogen Saturation in Northern Forest Ecosystems, BioScience, 39(6), 378–386, doi:10.2307/1311067, 1989.

Alexander, B., Park, R. J., Jacob, D. J., Li, Q. B., Yantosca, R. M., Savarino, J., Lee, C. C. W. and Thiemens, M. H.: Sulfate formation in sea-salt aerosols: Constraints from oxygen isotopes, J. Geophys. Res. Atmospheres, 110(D10), D10307, doi:10.1029/2004JD005659, 2005.

Alexander, B., Park, R. J., Jacob, D. J. and Gong, S.: Transition metal-catalyzed oxidation of atmospheric sulfur: Global implications for the sulfur budget, J. Geophys. Res., 114(D2), doi:10.1029/2008JD010486, 2009.

Alexander, B., Allman, D. J., Amos, H. M., Fairlie, T. D., Dachs, J., Hegg, D. A. and Sletten, R. S.: Isotopic constraints on the formation pathways of sulfate aerosol in the marine boundary layer of the subtropical northeast Atlantic Ocean, J. Geophys. Res. Atmospheres, 117(D6), D06304, doi:10.1029/2011JD016773, 2012.

Amos, H. M., Jacob, D. J., Holmes, C. D., Fisher, J. A., Wang, Q., Yantosca, R. M., Corbitt, E. S., Galarneau, E., Rutter, A. P., Gustin, M. S., Steffen, A., Schauer, J. J., Graydon, J. A., Louis, V. L. St., Talbot, R. W., Edgerton, E. S., Zhang, Y. and Sunderland, E. M.: Gas-particle partitioning of atmospheric Hg(II) and its effect on global mercury deposition, Atmos. Chem. Phys., 12(1), 591–603, doi:10.5194/acp-12-591-2012, 2012.

Andreae, M. O., Talbot, R. W., Berresheim, H. and Beecher, K. M.: Precipitation chemistry in central Amazonia, J. Geophys. Res., 95(D10), 16987, doi:10.1029/JD095iD10p16987, 1990.

Arlander, D. W., Cronn, D. R., Farmer, J. C., Menzia, F. A. and Westberg, H. H.: Gaseous oxygenated hydrocarbons in the remote marine troposphere, J. Geophys. Res., 95(D10), 16391, doi:10.1029/JD095iD10p16391, 1990.

Ayers, G. P. and Gillett, R. W.: First observations of cloud water acidity in tropical Australia, Clean Air Aust, 22(2), 53–57, 1988.

Baboukas, E. D., Kanakidou, M. and Mihalopoulos, N.: Carboxylic acids in gas and particulate phase above the Atlantic Ocean, J. Geophys. Res. Atmospheres, 105(D11), 14459–14471, doi:10.1029/1999JD900977, 2000.

Benedict, K. B., Lee, T. and Collett, J. L.: Cloud water composition over the southeastern Pacific Ocean during the VOCALS regional experiment, Atmos. Environ., 46, 104–114, doi:10.1016/j.atmosenv.2011.10.029, 2012.

Błaś, M., Polkowska, Ż., Sobik, M., Klimaszewska, K., Nowiński, K. and Namieśnik, J.: Fog water chemical composition in different geographic regions of Poland, Atmospheric Res., 95(4), 455–469, doi:10.1016/j.atmosres.2009.11.008, 2010.

Boris, A. J., Lee, T., Park, T., Choi, J., Seo, S. J. and Collett Jr., J. L.: Fog composition at Baengnyeong Island in the eastern Yellow Sea: detecting markers of aqueous atmospheric oxidations, Atmos.Chem. Phys., 16(2), 437–453, doi:10.5194/acp-16-437-2016, 2016.

Bormann, B. T., Tarrant, R. F., McClellan, M. H. and Savage, T.: Chemistry of Rainwater and Cloud Water at Remote Sites in Alaska and Oregon, J. Environ. Qual., 18(2), 149, doi:10.2134/jeq1989.00472425001800020003x, 1989.

Bouwman, A. F., Lee, D. S., Asman, W. A. H., Dentener, F. J., Van Der Hoek, K. W. and Olivier, J. G. J.: A global high-resolution emission inventory for ammonia, Glob. Biogeochem. Cycles, 11(4), 561–587, doi:10.1029/97GB02266, 1997.

Bouwman, A. F., Van Vuuren, D. P., Derwent, R. G. and Posch, M.: A global analysis of acidification and eutrophication of terrestrial ecosystems, Water. Air. Soil Pollut., 141(1/4), 349–382, doi:10.1023/A:1021398008726, 2002.

Breider, T. J., Mickley, L. J., Jacob, D. J., Ge, C., Wang, J., Payer Sulprizio, M., Croft, B., Ridley, D. A., McConnell, J. R., Sharma, S., Husain, L., Dutkiewicz, V. A., Eleftheriadis, K., Skov, H. and Hopke, P. K.: Multidecadal trends in aerosol radiative forcing over the Arctic: Contribution of changes in anthropogenic aerosol to Arctic warming since 1980: The 1980-2010 Trends in Arctic Aerosol RF, J. Geophys. Res. Atmospheres, 122(6), 3573–3594, doi:10.1002/2016JD025321, 2017.

Budhavant, K. B., Rao, P. S. P., Safai, P. D., Granat, L. and Rodhe, H.: Chemical composition of the inorganic fraction of cloud-water at a high altitude station in West India, Atmos. Environ., 88, 59–65, doi:10.1016/j.atmosenv.2014.01.039, 2014.

Calvert, J. G., Lazrus, A., Kok, G. L., Heikes, B. G., Walega, J. G., Lind, J. and Cantrell, C. A.: Chemical mechanisms of acid generation in the troposphere, Nature, 317(6032), 27–35, doi:10.1038/317027a0, 1985.

Carmichael, G. R., Peters, L. K. and Saylor, R. D.: The STEM-II regional scale acid deposition and photochemical oxidant model—I. An overview of model development and applications, Atmos. Environ. Part Gen. Top., 25(10), 2077–2090, doi:10.1016/0960-1686(91)90085-L, 1991.

Castillo, R. A., Jiusto, J. E. and Mclaren, E.: The pH and ionic composition of stratiform cloud water, Atmos. Environ. 1967, 17(8), 1497–1505, doi:10.1016/0004-6981(83)90303-7, 1983.

Chang, J. S., Brost, R. A., Isaksen, I. S. A., Madronich, S., Middleton, P., Stockwell, W. R. and Walcek, C. J.: A three-dimensional Eulerian acid deposition model: Physical concepts and formulation, J. Geophys. Res., 92(D12), 14681, doi:10.1029/JD092iD12p14681, 1987.

Chen, Q., Schmidt, J. A., Shah, V., Jaeglé, L., Sherwen, T. and Alexander, B.: Sulfate production by reactive bromine: Implications for the global sulfur and reactive bromine budgets, Geophys. Res. Lett., 44(13), 7069–7078, doi:10.1002/2017GL073812, 2017.

Chen, Y., Xie, S., Luo, B. and Zhai, C.: Particulate pollution in urban Chongqing of southwest China: Historical trends of variation, chemical characteristics and source apportionment, Sci. Total Environ., 584–585, 523–534, doi:10.1016/j.scitotenv.2017.01.060, 2017.

Collett, J. L., Oberholzer, B., Mosimann, L., Staehelin, J. and Waldvogel, A.: Contributions of cloud processes to precipitation chemistry in mixed phase clouds, Water. Air. Soil Pollut., 68(1–2), 43–57, doi:10.1007/BF00479392, 1993.

Collett, J. L., Hoag, K. J., Rao, X. and Pandis, S. N.: Internal acid buffering in San Joaquin Valley fog drops and its influence on aerosol processing, Atmos. Environ., 33(29), 4833–4847, doi:10.1016/S1352-2310(99)00221-6, 1999.

Deguillaume, L., Charbouillot, T., Joly, M., Vaïtilingom, M., Parazols, M., Marinoni, A., Amato, P., Delort, A.-M., Vinatier, V., Flossmann, A., Chaumerliac, N., Pichon, J. M., Houdier, S., Laj, P., Sellegri, K., Colomb, A., Brigante, M. and Mailhot, G.: Classification of clouds sampled at the puy de Dôme (France) based on 10 yr of monitoring of their physicochemical properties, Atmos. Chem. Phys., 14(3), 1485–1506, doi:10.5194/acp-14-1485-2014, 2014.

Dentener, F. J. and Crutzen, P. J.: A three-dimensional model of the global ammonia cycle, J. Atmospheric Chem., 19(4), 331–369, doi:10.1007/BF00694492, 1994.

van Donkelaar, A., Martin, R. V., Leaitch, W. R., Macdonald, A. M., Walker, T. W., Streets, D. G., Zhang, Q., Dunlea, E. J., Jimenez, J. L., Dibb, J. E., Huey, L. G., Weber, R. and Andreae, M. O.: Analysis of aircraft and satellite measurements from

the Intercontinental Chemical Transport Experiment (INTEX-B) to quantify long-range transport of East Asian sulfur to Canada, Atmos. Chem. Phys., 8(11), 2999–3014, doi:10.5194/acp-8-2999-2008, 2008.

Driscoll, C. T., Lawrence, G. B., Bulger, A. J., Butler, T. J., Cronan, C. S., Eagar, C., Lambert, K. F., Likens, G. E., Stoddard, J. L. and Weathers, K. C.: Acidic Deposition in the Northeastern United States: Sources and Inputs, Ecosystem Effects, and Management Strategies, BioScience, 51(3), 180, doi:10.1641/0006-3568(2001)051[0180:ADITNU]2.0.CO;2, 2001.

Duan, L., Yu, Q., Zhang, Q., Wang, Z., Pan, Y., Larssen, T., Tang, J. and Mulder, J.: Acid deposition in Asia: Emissions, deposition, and ecosystem effects, Atmos. Environ., 146, 55–69, doi:10.1016/j.atmosenv.2016.07.018, 2016.

EANET: The Third Periodic Report on the State of Acid Deposition in East Asia. Part II: National Assessments. [online] Available from: https://www.eanet.asia/wp-content/uploads/2019/03/3_PRSAD2.pdf (Accessed 30 March 2020), 2016.

EANET: EANET Data on the Acid Deposition in the East Asian Region, [online] Available from: https://monitoring.eanet.asia/document/public/index (Accessed 9 October 2019), 2019.

ECCC: Monitoring of Atmospheric Precipitation Chemistry, [online] Available from: http://donnees.ec.gc.ca/data/air/monitor/monitoring-of-atmospheric-precipitation-chemistry/?lang=en (Accessed 18 October 2019), 2018.

EEA: National Emission Ceilings (NEC) Directive emission inventory data, [online] Available from: https://www.eea.europa.eu/data-and-maps/data/national-emission-ceilings-nec-directive-inventory-16 (Accessed 15 November 2019), 2019.

EMEP: EMEP measurement data online, [online] Available from: https://projects.nilu.no//ccc/emepdata.html (Accessed 1 April 2020), 2015.

Engelbrecht, J. P., Moosmüller, H., Pincock, S., Jayanty, R. K. M., Lersch, T. and Casuccio, G.: Technical note: Mineralogical, chemical, morphological, and optical interrelationships of mineral dust re-suspensions, Atmos. Chem. Phys., 16(17), 10809–10830, doi:10.5194/acp-16-10809-2016, 2016.

Ervens, B., Turpin, B. J. and Weber, R. J.: Secondary organic aerosol formation in cloud droplets and aqueous particles (aqSOA): a review of laboratory, field and model studies, Atmos. Chem. Phys., 11(21), 11069–11102, doi:10.5194/acp-11-11069-2011, 2011.

Ervens, B., Wang, Y., Eagar, J., Leaitch, W. R., Macdonald, A. M., Valsaraj, K. T. and Herckes, P.: Dissolved organic carbon (DOC) and select aldehydes in cloud and fog water: the role of the aqueous phase in impacting trace gas budgets, Atmos. Chem. Phys., 13(10), 5117–5135, doi:10.5194/acp-13-5117-2013, 2013.

Eyring, V., Köhler, H. W., van Aardenne, J. and Lauer, A.: Emissions from international shipping: 1. The last 50 years, J. Geophys. Res. Atmospheres, 110(D17), D17305, doi:10.1029/2004JD005619, 2005.

Fairlie, T. D., Jacob, D. J. and Park, R. J.: The impact of transpacific transport of mineral dust in the United States, Atmos. Environ., 41(6), 1251–1266, doi:10.1016/j.atmosenv.2006.09.048, 2007.

Fernández-González, R., Yebra-Pimentel, I., Martínez-Carballo, E., Simal-Gándara, J. and Pontevedra-Pombal, X.: Atmospheric pollutants in fog and rain events at the northwestern mountains of the Iberian Peninsula, Sci. Total Environ., 497–498, 188–199, doi:10.1016/j.scitotenv.2014.07.093, 2014.

Fisak, J., Stoyanova, V., Tesar, M., Petrova, P., Daskalova, N., Tsacheva, T. and Marinov, M.: The pollutants in rime and fog water and in air at Milesovka Observatory (Czech Republic), Biologia (Bratisl.), 64(3), doi:10.2478/s11756-009-0080-0, 2009.

Fisher, J. A., Jacob, D. J., Wang, Q., Bahreini, R., Carouge, C. C., Cubison, M. J., Dibb, J. E., Diehl, T., Jimenez, J. L., Leibensperger, E. M., Lu, Z., Meinders, M. B. J., Pye, H. O. T., Quinn, P. K., Sharma, S., Streets, D. G., van Donkelaar, A. and Yantosca, R. M.: Sources, distribution, and acidity of sulfate–ammonium aerosol in the Arctic in winter–spring, Atmos. Environ., 45(39), 7301–7318, doi:10.1016/j.atmosenv.2011.08.030, 2011.

Franco, B., Clarisse, L., Stavrakou, T., Müller, J. -F., Taraborrelli, D., Hadji-Lazaro, J., Hannigan, J. W., Hase, F., Hurtmans, D., Jones, N., Lutsch, E., Mahieu, E., Ortega, I., Schneider, M., Strong, K., Vigouroux, C., Clerbaux, C. and Coheur, P. -F.: Spaceborne Measurements of Formic and Acetic Acids: A Global View of the Regional Sources, Geophys. Res. Lett., 47(4), doi:10.1029/2019GL086239, 2020.

Galloway, J. N.: Acid deposition: Perspectives in time and space, Water. Air. Soil Pollut., 85(1), 15–24, doi:10.1007/BF00483685, 1995.

Gelaro, R., McCarty, W., Suárez, M. J., Todling, R., Molod, A., Takacs, L., Randles, C. A., Darmenov, A., Bosilovich, M. G., Reichle, R., Wargan, K., Coy, L., Cullather, R., Draper, C., Akella, S., Buchard, V., Conaty, A., da Silva, A. M., Gu, W., Kim, G.-K., Koster, R., Lucchesi, R., Merkova, D., Nielsen, J. E., Partyka, G., Pawson, S., Putman, W., Rienecker, M., Schubert, S. D., Sienkiewicz, M. and Zhao, B.: The Modern-Era Retrospective Analysis for Research and Applications, Version 2 (MERRA-2), J. Clim., 30(14), 5419–5454, doi:10.1175/JCLI-D-16-0758.1, 2017.

Gillett, R. W. and Ayers, G. P.: Maritime Cloudwater Acidity Near Tasmania, Clean Air Aust, 23, 106–109, 1989.

Gioda, A., Reyes-Rodríguez, G. J., Santos-Figueroa, G., Collett, J. L., Decesari, S., Ramos, M. da C. K. V., Bezerra Netto, H. J. C., de Aquino Neto, F. R. and Mayol-Bracero, O. L.: Speciation of water-soluble inorganic, organic, and total nitrogen in a background marine environment: Cloud water, rainwater, and aerosol particles, J. Geophys. Res., 116(D5), doi:10.1029/2010JD015010, 2011.

von Glasow, R. and Crutzen, P. J.: Tropospheric Halogen Chemistry, in Treatise on Geochemistry, pp. 1–67, Elsevier., 2003.

Graedel, T. E. and Goldberg, K. I.: Kinetic studies of raindrop chemistry: 1. Inorganic and organic processes, J. Geophys. Res., 88(C15), 10865, doi:10.1029/JC088iC15p10865, 1983.

Guenther, A. B., Jiang, X., Heald, C. L., Sakulyanontvittaya, T., Duhl, T., Emmons, L. K. and Wang, X.: The Model of Emissions of Gases and Aerosols from Nature version 2.1 (MEGAN2.1): an extended and updated framework for modeling biogenic emissions, Geosci. Model Dev., 5(6), 1471–1492, doi:10.5194/gmd-5-1471-2012, 2012.

Gundersen, P., Schmidt, I. K. and Raulund-Rasmussen, K.: Leaching of nitrate from temperate forests: effects of air pollution and forest management, Environ. Rev., 14(1), 1–57, doi:10.1139/a05-015, 2006.

Guo, J., Wang, Y., Shen, X., Wang, Z., Lee, T., Wang, X., Li, P., Sun, M., Collett, J. L., Wang, W. and Wang, T.: Characterization of cloud water chemistry at Mount Tai, China: Seasonal variation, anthropogenic impact, and cloud processing, Atmos. Environ., 60, 467–476, doi:10.1016/j.atmosenv.2012.07.016, 2012.

Hass, H., Ebel, A., Feldmann, H., Jakobs, H. J. and Memmesheimer, M.: Evaluation studies with a regional chemical transport model (EURAD) using air quality data from the EMEP monitoring network, Atmos. Environ. Part Gen. Top., 27(6), 867–887, doi:10.1016/0960-1686(93)90007-L, 1993.

Heald, C. L., Jacob, D. J., Turquety, S., Hudman, R. C., Weber, R. J., Sullivan, A. P., Peltier, R. E., Atlas, E. L., de Gouw, J. A., Warneke, C., Holloway, J. S., Neuman, J. A., Flocke, F. M. and Seinfeld, J. H.: Concentrations and sources of organic carbon aerosols in the free troposphere over North America, J. Geophys. Res. Atmospheres, 111(D23), D23S47, doi:10.1029/2006JD007705, 2006.

Hegg, D. A., Hobbs, P. V. and Radke, L. F.: Measurements of the scavenging of sulfate and nitrate in clouds, Atmos. Environ. 1967, 18(9), 1939–1946, doi:10.1016/0004-6981(84)90371-8, 1984.

Helas, G., Bingemer, H. and Andreae, M. O.: Organic acids over equatorial Africa: Results from DECAFE 88, J. Geophys. Res., 97(D6), 6187, doi:10.1029/91JD01438, 1992.

Herrmann, H., Schaefer, T., Tilgner, A., Styler, S. A., Weller, C., Teich, M. and Otto, T.: Tropospheric Aqueous-Phase Chemistry: Kinetics, Mechanisms, and Its Coupling to a Changing Gas Phase, Chem. Rev., 115(10), 4259–4334, doi:10.1021/cr500447k, 2015.

Hill, K. A., Shepson, P. B., Galbavy, E. S., Anastasio, C., Kourtev, P. S., Konopka, A. and Stirm, B. H.: Processing of atmospheric nitrogen by clouds above a forest environment, J. Geophys. Res., 112(D11), D11301, doi:10.1029/2006JD008002, 2007.

Hoesly, R. M., Smith, S. J., Feng, L., Klimont, Z., Janssens-Maenhout, G., Pitkanen, T., Seibert, J. J., Vu, L., Andres, R. J., Bolt, R. M., Bond, T. C., Dawidowski, L., Kholod, N., Kurokawa, J.-I., Li, M., Liu, L., Lu, Z., Moura, M. C. P., O'Rourke, P. R. and Zhang, Q.: Historical (1750–2014) anthropogenic emissions of reactive gases and aerosols from the Community Emissions Data System (CEDS), Geosci. Model Dev., 11(1), 369–408, doi:10.5194/gmd-11-369-2018, 2018.

Holmes, C. D., Prather, M. J. and Vinken, G. C. M.: The climate impact of ship NO$_x$ emissions: an improved estimate accounting for plume chemistry, Atmos. Chem. Phys., 14(13), 6801–6812, doi:10.5194/acp-14-6801-2014, 2014.

Holmes, C. D., Bertram, T. H., Confer, K. L., Graham, K. A., Ronan, A. C., Wirks, C. K. and Shah, V.: The Role of Clouds in the Tropospheric NO$_x$ Cycle: A New Modeling Approach for Cloud Chemistry and Its Global Implications, Geophys. Res. Lett., 46(9), 4980–4990, doi:10.1029/2019GL081990, 2019.

Hu, L., Millet, D. B., Baasandorj, M., Griffis, T. J., Turner, P., Helmig, D., Curtis, A. J. and Hueber, J.: Isoprene emissions and impacts over an ecological transition region in the U.S. Upper Midwest inferred from tall tower measurements: Isoprene emissions in US Upper Midwest, J. Geophys. Res. Atmospheres, 120(8), 3553–3571, doi:10.1002/2014JD022732, 2015.

Huang, J., Jaeglé, L. and Shah, V.: Using CALIOP to constrain blowing snow emissions of sea salt aerosols over Arctic and Antarctic sea ice, Atmos. Chem. Phys., 18(22), 16253–16269, doi:10.5194/acp-18-16253-2018, 2018.

Hudman, R. C., Moore, N. E., Mebust, A. K., Martin, R. V., Russell, A. R., Valin, L. C. and Cohen, R. C.: Steps towards a mechanistic model of global soil nitric oxide emissions: implementation and space based-constraints, Atmos. Chem. Phys., 12(16), 7779–7795, doi:10.5194/acp-12-7779-2012, 2012.

Huijnen, V., Williams, J., van Weele, M., van Noije, T., Krol, M., Dentener, F., Segers, A., Houweling, S., Peters, W., de Laat, J., Boersma, F., Bergamaschi, P., van Velthoven, P., Le Sager, P., Eskes, H., Alkemade, F., Scheele, R., Nédélec, P. and Pätz, H.-W.: The global chemistry transport model TM5: description and evaluation of the tropospheric chemistry version 3.0, Geosci. Model Dev., 3(2), 445–473, doi:10.5194/gmd-3-445-2010, 2010.

Hutchings, J. W., Robinson, M. S., McIlwraith, H., Triplett Kingston, J. and Herckes, P.: The Chemistry of Intercepted Clouds in Northern Arizona during the North American Monsoon Season, Water. Air. Soil Pollut., 199(1–4), 191–202, doi:10.1007/s11270-008-9871-0, 2009.

Jaeglé, L., Quinn, P. K., Bates, T. S., Alexander, B. and Lin, J.-T.: Global distribution of sea salt aerosols: new constraints from in situ and remote sensing observations, Atmos. Chem. Phys., 11(7), 3137–3157, doi:10.5194/acp-11-3137-2011, 2011.

Kawamura, K., Steinberg, S. and Kaplan, I. R.: Concentrations of monocar☐ylic and dicar☐ylic acids and aldehydes in southern California wet precipitations: Comparison of urban and nonurban samples and compositional changes during scavenging, Atmos. Environ., 30(7), 1035–1052, doi:10.1016/1352-2310(95)00404-1, 1996.

Keene, W. C. and Galloway, J. N.: Organic acidity in precipitation of North America, Atmospheric Environ. 1967, 18(11), 2491–2497, doi:10.1016/0004-6981(84)90020-9, 1984.

Keene, W. C., Galloway, J. N. and Holden, J. D.: Measurement of weak organic acidity in precipitation from remote areas of the world, J. Geophys. Res. Oceans, 88(C9), 5122–5130, doi:10.1029/JC088iC09p05122, 1983.

Keene, W. C., Galloway, J. N., Likens, G. E., Deviney, F. A., Mikkelsen, K. N., Moody, J. L. and Maben, J. R.: Atmospheric Wet Deposition in Remote Regions: Benchmarks for Environmental Change, J. Atmospheric Sci., 72(8), 2947–2978, doi:10.1175/JAS-D-14-0378.1, 2015.

Keller, C. A., Long, M. S., Yantosca, R. M., Da Silva, A. M., Pawson, S. and Jacob, D. J.: HEMCO v1.0: a versatile, ESMF-compliant component for calculating emissions in atmospheric models, Geosci. Model Dev., 7(4), 1409–1417, doi:10.5194/gmd-7-1409-2014, 2014.

Khan, M. A. H., Lyons, K., Chhantyal-Pun, R., McGillen, M. R., Caravan, R. L., Taatjes, C. A., Orr-Ewing, A. J., Percival, C. J. and Shallcross, D. E.: Investigating the Tropospheric Chemistry of Acetic Acid Using the Global 3-D Chemistry Transport Model, STOCHEM-CRI, J. Geophys. Res. Atmospheres, 123(11), 6267–6281, doi:10.1029/2018JD028529, 2018.

Khare, P., Kumar, N., Kumari, K. M. and Srivastava, S. S.: Atmospheric formic and acetic acids: An overview, Rev. Geophys., 37(2), 227–248, doi:10.1029/1998RG900005, 1999.

Kim, H. J., Lee, T., Park, T., Park, G., Collett, J. L., Park, K., Ahn, J. Y., Ban, J., Kang, S., Kim, K., Park, S.-M., Jho, E. H. and Choi, Y.: Ship-borne observations of sea fog and rain chemistry over the North and South Pacific Ocean, J. Atmos. Chem., 76(4), 315–326, doi:10.1007/s10874-020-09403-8, 2019.

Kim, P. S., Jacob, D. J., Fisher, J. A., Travis, K., Yu, K., Zhu, L., Yantosca, R. M., Sulprizio, M. P., Jimenez, J. L., Campuzano-Jost, P., Froyd, K. D., Liao, J., Hair, J. W., Fenn, M. A., Butler, C. F., Wagner, N. L., Gordon, T. D., Welti, A., Wennberg, P. O., Crounse, J. D., St. Clair, J. M., Teng, A. P., Millet, D. B., Schwarz, J. P., Markovic, M. Z. and Perring, A. E.: Sources, seasonality, and trends of southeast US aerosol: an integrated analysis of surface, aircraft, and satellite observations with the GEOS-Chem chemical transport model, Atmos. Chem. Phys., 15(18), 10411–10433, doi:10.5194/acp-15-10411-2015, 2015.

Kuylenstierna, J. C. I., Rodhe, H., Cinderby, S. and Hicks, K.: Acidification in Developing Countries: Ecosystem Sensitivity and the Critical Load Approach on a Global Scale, AMBIO J. Hum. Environ., 30(1), 20–28, doi:10.1579/0044-7447-30.1.20, 2001.

Lamarque, J.-F., Emmons, L. K., Hess, P. G., Kinnison, D. E., Tilmes, S., Vitt, F., Heald, C. L., Holland, E. A., Lauritzen, P. H., Neu, J., Orlando, J. J., Rasch, P. J. and Tyndall, G. K.: CAM-chem: description and evaluation of interactive atmospheric chemistry in the Community Earth System Model, Geosci. Model Dev., 5(2), 369–411, doi:10.5194/gmd-5-369-2012, 2012.

Lamarque, J.-F., Dentener, F., McConnell, J., Ro, C.-U., Shaw, M., Vet, R., Bergmann, D., Cameron-Smith, P., Dalsoren, S., Doherty, R., Faluvegi, G., Ghan, S. J., Josse, B., Lee, Y. H., MacKenzie, I. A., Plummer, D., Shindell, D. T., Skeie, R. B., Stevenson, D. S., Strode, S., Zeng, G., Curran, M., Dahl-Jensen, D., Das, S., Fritzsche, D. and Nolan, M.: Multi-model mean

nitrogen and sulfur deposition from the Atmospheric Chemistry and Climate Model Intercomparison Project (ACCMIP): evaluation of historical and projected future changes, Atmos. Chem. Phys., 13(16), 7997–8018, doi:10.5194/acp-13-7997-2013, 2013.

Langner, J., Bergström, R. and Foltescu, V.: Impact of climate change on surface ozone and deposition of sulphur and nitrogen in Europe, Atmos. Environ., 39(6), 1129–1141, doi:10.1016/j.atmosenv.2004.09.082, 2005.

Legrand, M., Preunkert, S., Jourdain, B. and Aumont, B.: Year-round records of gas and particulate formic and acetic acids in the boundary layer at Dumont d'Urville, coastal Antarctica, J. Geophys. Res. Atmospheres, 109(D6), D06313, doi:10.1029/2003JD003786, 2004.

Li, J., Wang, X., Chen, J., Zhu, C., Li, W., Li, C., Liu, L., Xu, C., Wen, L., Xue, L., Wang, W., Ding, A. and Herrmann, H.: Chemical composition and droplet size distribution of cloud at the summit of Mount Tai, China, Atmos. Chem. Phys., 17(16), 9885–9896, doi:10.5194/acp-17-9885-2017, 2017.

Li, M., Zhang, Q., Kurokawa, J.-I., Woo, J.-H., He, K., Lu, Z., Ohara, T., Song, Y., Streets, D. G., Carmichael, G. R., Cheng, Y., Hong, C., Huo, H., Jiang, X., Kang, S., Liu, F., Su, H. and Zheng, B.: MIX: a mosaic Asian anthropogenic emission inventory under the international collaboration framework of the MICS-Asia and HTAP, Atmos. Chem. Phys., 17(2), 935–963, doi:10.5194/acp-17-935-2017, 2017.

Li, T., Wang, Z., Wang, Y., Wu, C., Liang, Y., Xia, M., Yu, C., Yun, H., Wang, W., Wang, Y., Guo, J., Herrmann, H. and Wang, T.: Chemical characteristics of cloud water and the impacts on aerosol properties at a subtropical mountain site in Hong Kong SAR, Atmos. Chem. Phys., 20(1), 391–407, doi:10.5194/acp-20-391-2020, 2020.

Liljestrand, H. M.: Average rainwater pH, concepts of atmospheric acidity, and buffering in open systems, Atmospheric Environ. 1967, 19(3), 487–499, doi:10.1016/0004-6981(85)90169-6, 1985.

Liu, H., Jacob, D. J., Bey, I. and Yantosca, R. M.: Constraints from 210Pb and 7Be on wet deposition and transport in a global three-dimensional chemical, J. Geophys. Res., 106(D11), 12109--12128, doi:10.1029/2000JD900839, 2001.

Mahowald, N. M., Baker, A. R., Bergametti, G., Brooks, N., Duce, R. A., Jickells, T. D., Kubilay, N., Prospero, J. M. and Tegen, I.: Atmospheric global dust cycle and iron inputs to the ocean, Glob. Biogeochem. Cycles, 19(4), GB4025, doi:10.1029/2004GB002402, 2005.

Makowski Giannoni, S., Rollenbeck, R., Fabian, P. and Bendix, J.: Complex topography influences atmospheric nitrate deposition in a neotropical mountain rainforest, Atmos. Environ., 79, 385–394, doi:10.1016/j.atmosenv.2013.06.023, 2013.

Makowski Giannoni, S., Trachte, K., Rollenbeck, R., Lehnert, L., Fuchs, J. and Bendix, J.: Atmospheric salt deposition in a tropical mountain rainforest at the eastern Andean slopes ofsouth Ecuador – Pacific or Atlantic origin?, Atmos. Chem. Phys., 16(15), 10241–10261, doi:10.5194/acp-16-10241-2016, 2016.

Mao, J., Paulot, F., Jacob, D. J., Cohen, R. C., Crounse, J. D., Wennberg, P. O., Keller, C. A., Hudman, R. C., Barkley, M. P. and Horowitz, L. W.: Ozone and organic nitrates over the eastern United States: Sensitivity to isoprene chemistry, J. Geophys. Res. Atmospheres, 118(19), 11,256-11,268, doi:10.1002/jgrd.50817, 2013.

Marais, E. A. and Wiedinmyer, C.: Air Quality Impact of Diffuse and Inefficient Combustion Emissions in Africa (DICE-Africa), Environ. Sci. Technol., 50(19), 10739–10745, doi:10.1021/acs.est.6b02602, 2016.

Martin, L. R., Damschen, D. E. and Judekis, H. S.: Sulfur oxide oxidation reaction in aqueous solution, US Environmental Protection Agency, Research Triangle Park, NC., 1981.

McDuffie, E. E., Fibiger, D. L., Dubé, W. P., Lopez-Hilfiker, F., Lee, B. H., Thornton, J. A., Shah, V., Jaeglé, L., Guo, H., Weber, R. J., Michael Reeves, J., Weinheimer, A. J., Schroder, J. C., Campuzano-Jost, P., Jimenez, J. L., Dibb, J. E., Veres, P., Ebben, C., Sparks, T. L., Wooldridge, P. J., Cohen, R. C., Hornbrook, R. S., Apel, E. C., Campos, T., Hall, S. R., Ullmann, K. and Brown, S. S.: Heterogeneous N2O5 Uptake During Winter: Aircraft Measurements During the 2015 WINTER Campaign and Critical Evaluation of Current Parameterizations, J. Geophys. Res. Atmospheres, 123(8), 4345–4372, doi:10.1002/2018JD028336, 2018.

Meyer-Christoffer, A., Becker, A., Finger, P., Schneider, U. and Ziese, M.: GPCC Climatology Version 2018 at 0.5°: Monthly Land-Surface Precipitation Climatology for Every Month and the Total Year from Rain-Gauges built on GTS-based and Historical Data, , doi:10.5676/DWD_GPCC/CLIM_M_V2018_050, 2018.

Michna, P., Werner, R. A. and Eugster, W.: Does fog chemistry in Switzerland change with altitude?, Atmos. Res., 151, 31–44, doi:10.1016/j.atmosres.2014.02.008, 2015.

Millet, D. B., Baasandorj, M., Farmer, D. K., Thornton, J. A., Baumann, K., Brophy, P., Chaliyakunnel, S., de Gouw, J. A., Graus, M., Hu, L., Koss, A., Lee, B. H., Lopez-Hilfiker, F. D., Neuman, J. A., Paulot, F., Peischl, J., Pollack, I. B., Ryerson, T. B., Warneke, C., Williams, B. J. and Xu, J.: A large and ubiquitous source of atmospheric formic acid, Atmos. Chem. Phys., 15(11), 6283–6304, doi:10.5194/acp-15-6283-2015, 2015.

Moch, J. M., Dovrou, L. J., Mickley, L. J., Keutsch, F. N., Liu, Z., Wang, Y., Dombek, T. L., Kuwata, M., Budisulistiorini, S. H., Yang, L., Decesari, S., Paglione, M., Alexander, B., Shao, J., Munger, J. W. and Jacob, D. J.: Global importance of hydroxymethanesulfonate in ambient particulate matter: Implications for air quality, J. Geophys. Res. Atmospheres, doi: 10.1029/2020JD032706, 2020. ~~Moch, J. M., Dovrou, L. J., Mickley, L. J., Keutsch, F. N., Liu, Z., Wang, Y., Dombek, T. L., Kuwata, M., Budisulistiorini, S. H., Yang, L., Decesari, S., Paglione, M., Alexander, B., Shao, J., Munger, J. W. and Jacob, D. J.: Global importance of hydroxymethanesulfonate in ambient particular matter: Implications for air quality., in review. Available from: http://acmg.seas.harvard.edu/publications/2020/moch_HMS_submitted_2020.pdf (Accessed 1 April 2020), 2020.~~

Morgan, J. J.: Factors Governing the pH, Availability of H+, and Oxidation Capacity of Rain, in Atmospheric Chemistry, edited by E. D. Goldberg, pp. 17–40, Springer Berlin Heidelberg, Berlin, Heidelberg., 1982.

Murray, L. T., Jacob, D. J., Logan, J. A., Hudman, R. C. and Koshak, W. J.: Optimized regional and interannual variability of lightning in a global chemical transport model constrained by LIS/OTD satellite data, J. Geophys. Res. Atmospheres, 117(D20), doi:10.1029/2012JD017934, 2012.

Murray, G. L. D., Kimball, K. D., Hill, L. B., Hislop, J. E. and Weathers, K. C.: Long-Term Trends in Cloud and Rain Chemistry on Mount Washington, New Hampshire, Water. Air. Soil Pollut., 224(9), doi:10.1007/s11270-013-1653-7, 2013.

Myriokefalitakis, S., Tsigaridis, K., Mihalopoulos, N., Sciare, J., Nenes, A., Kawamura, K., Segers, A. and Kanakidou, M.: In-cloud oxalate formation in the global troposphere: a 3-D modeling study, Atmos. Chem. Phys., 11(12), 5761–5782, doi:10.5194/acp-11-5761-2011, 2011.

NADP: NTN data for all sites, [online] Available from: http://nadp.slh.wisc.edu/data/NTN/ntnAllsites.aspx (Accessed 11 October 2019), 2019.

Nieberding, F., Breuer, B., Braeckevelt, E., Klemm, O., Song, Q. and Zhang, Y.: Fog Water Chemical Composition on Ailaoshan Mountain, Yunnan Province, SW China, Aerosol Air Qual. Res., 18(1), 37–48, doi:10.4209/aaqr.2017.01.0060, 2018.

Niu, Y., Li, X., Pu, J. and Huang, Z.: Organic acids contribute to rainwater acidity at a rural site in eastern China, Air Qual. Atmosphere Health, 11(4), 459–469, doi:10.1007/s11869-018-0553-9, 2018.

Nordstrom, D. K., Plummer, L. N., Langmuir, D., Busenberg, E., May, H. M., Jones, B. F. and Parkhurst, D. L.: Revised Chemical Equilibrium Data for Major Water—Mineral Reactions and Their Limitations, in Chemical Modeling of Aqueous Systems II, vol. 416, edited by D. C. Melchior and R. L. Bassett, pp. 398–413, American Chemical Society, Washington, DC., 1990.

NRC: Acid Deposition: Atmospheric Processes in Eastern North America, National Academies Press, Washington, D.C., 1983.

Ogren, J. and Rodhe, H.: Measurements of the chemical composition of cloudwater at a clean air site in central Scandinavia, Tellus B Chem. Phys. Meteorol., 38(3–4), 190–196, doi:10.3402/tellusb.v38i3-4.15128, 1986.

Olendrzynski, K., Jonson, J. E., Bartnicki, J., Jakobsen, H. A. and Berge, E.: EMEP Eulerian model for acid deposition over Europe, Int. J. Environ. Pollut., 14(1/2/3/4/5/6), 391, doi:10.1504/IJEP.2000.000561, 2000.

Overton, J. H., Aneja, V. P. and Durham, J. L.: Production of sulfate in rain and raindrops in polluted atmospheres, Atmos. Environ. 1967, 13(3), 355–367, doi:10.1016/0004-6981(79)90292-0, 1979.

Pandis, S. N. and Seinfeld, J. H.: Sensitivity analysis of a chemical mechanism for aqueous-phase atmospheric chemistry, J. Geophys. Res., 94(D1), 1105--1126, doi:10.1029/JD094iD01p01105, 1989.

Parungo, F., Nagamoto, C., Nolt, I., Dias, M. and Nickerson, E.: Chemical analysis of cloud water collected over Hawaii, J. Geophys. Res., 87(C11), 8805, doi:10.1029/JC087iC11p08805, 1982.

Paulot, F., Wunch, D., Crounse, J. D., Toon, G. C., Millet, D. B., DeCarlo, P. F., Vigouroux, C., Deutscher, N. M., González Abad, G., Notholt, J., Warneke, T., Hannigan, J. W., Warneke, C., de Gouw, J. A., Dunlea, E. J., De Mazière, M., Griffith, D. W. T., Bernath, P., Jimenez, J. L. and Wennberg, P. O.: Importance of secondary sources in the atmospheric budgets of formic and acetic acids, Atmos. Chem. Phys., 11(5), 1989–2013, doi:10.5194/acp-11-1989-2011, 2011.

Paulot, F., Malyshev, S., Nguyen, T., Crounse, J. D., Shevliakova, E. and Horowitz, L. W.: Representing sub-grid scale variations in nitrogen deposition associated with land use in a global Earth system model: implications for present and future nitrogen deposition fluxes over North America, Atmos. Chem. Phys., 18(24), 17963–17978, doi:10.5194/acp-18-17963-2018, 2018.

Peña, R. M., García, S., Herrero, C., Losada, M., Vázquez, A. and Lucas, T.: Organic acids and aldehydes in rainwater in a northwest region of Spain, Atmos. Environ., 36(34), 5277–5288, doi:10.1016/S1352-2310(02)00648-9, 2002.

Philip, S., Martin, R. V., Snider, G., Weagle, C. L., van Donkelaar, A., Brauer, M., Henze, D. K., Klimont, Z., Venkataraman, C., Guttikunda, S. K. and Zhang, Q.: Anthropogenic fugitive, combustion and industrial dust is a significant, underrepresented fine particulate matter source in global atmospheric models, Environ. Res. Lett., 12(4), 044018, doi:10.1088/1748-9326/aa65a4, 2017.

Platt, U. and Hönninger, G.: The role of halogen species in the troposphere, Chemosphere, 52(2), 325–338, doi:10.1016/S0045-6535(03)00216-9, 2003.

Prabhakar, G., Ervens, B., Wang, Z., Maudlin, L. C., Coggon, M. M., Jonsson, H. H., Seinfeld, J. H. and Sorooshian, A.: Sources of nitrate in stratocumulus cloud water: Airborne measurements during the 2011 E-PEACE and 2013 NiCE studies, Atmos. Environ., 97, 166–173, doi:10.1016/j.atmosenv.2014.08.019, 2014.

Pye, H. O. T., Nenes, A., Alexander, B., Ault, A. P., Barth, M. C., Clegg, S. L., Collett Jr., J. L., Fahey, K. M., Hennigan, C. J., Herrmann, H., Kanakidou, M., Kelly, J. T., Ku, I.-T., McNeill, V. F., Riemer, N., Schaefer, T., Shi, G., Tilgner, A., Walker, J. T., Wang, T., Weber, R., Xing, J., Zaveri, R. A. and Zuend, A.: The acidity of atmospheric particles and clouds, Atmos. Chem. Phys., 20(8), 4809–4888, doi:10.5194/acp-20-4809-2020, 2020.

Reuss, J. O. and Johnson, D. W.: Acid Deposition and the Acidification of Soils and Waters, Springer New York, New York, NY., 1986.

Ridley, D. A., Heald, C. L., Pierce, J. R. and Evans, M. J.: Toward resolution-independent dust emissions in global models: Impacts on the seasonal and spatial distribution of dust., Geophys. Res. Lett., 40(11), 2873–2877, doi:10.1002/grl.50409, 2013.

Rodhe, H., Langner, J., Gallardo, L. and Kjellström, E.: Global scale transport of acidifying pollutants, Water. Air. Soil Pollut., 85(1), 37–50, doi:10.1007/BF00483687, 1995.

Rodhe, H., Dentener, F. and Schulz, M.: The Global Distribution of Acidifying Wet Deposition, Environ. Sci. Technol., 36(20), 4382–4388, doi:10.1021/es020057g, 2002.

Sander, R.: Compilation of Henry's law constants (version 4.0) for water as solvent, Atmos. Chem. Phys., 15(8), 4399–4981, doi:10.5194/acp-15-4399-2015, 2015.

Sanhueza, E., Arias, M. C., Donoso, L., Graterol, N., Hermoso, M., Marti, I., Romero, J., Rondon, A. and Santana, M.: Chemical composition of acid rains in the Venezuelan savannah region, Tellus B, 44(1), 54–62, doi:10.1034/j.1600-0889.1992.00005.x, 1992.

Saxena, V. K. and Lin, N.-H.: Cloud chemistry measurements and estimates of acidic deposition on an above cloudbase coniferous forest, Atmos. Environ. Part Gen. Top., 24(2), 329–352, doi:10.1016/0960-1686(90)90113-2, 1990.

Schunk, C., Trautwein, P., Hruschka, H., Frost, E., Dodson, L., Derhem, A., Bargach, J. and Menzel, A.: Testing Water Yield, Efficiency of Different Meshes and Water Quality with a Novel Fog Collector for High Wind Speeds, Aerosol Air Qual. Res., 18(1), 240–253, doi:10.4209/aaqr.2016.12.0528, 2018.

Schwab, J. J., Casson, P., Brandt, R., Husain, L., Dutkewicz, V., Wolfe, D., Demerjian, K. L., Civerolo, K. L., Rattigan, O. V., Felton, H. D. and Dukett, J. E.: Atmospheric Chemistry Measurements at Whiteface Mountain, NY: Cloud Water Chemistry, Precipitation Chemistry, and Particulate Matter, Aerosol Air Qual. Res., 16(3), 841–854, doi:10.4209/aaqr.2015.05.0344, 2016.

Sherwen, T., Schmidt, J. A., Evans, M. J., Carpenter, L. J., Großmann, K., Eastham, S. D., Jacob, D. J., Dix, B., Koenig, T. K., Sinreich, R., Ortega, I., Volkamer, R., Saiz-Lopez, A., Prados-Roman, C., Mahajan, A. S. and Ordóñez, C.: Global impacts of tropospheric halogens (Cl, Br, I) on oxidants and composition in GEOS-Chem, Atmos. Chem. Phys., 16(18), 12239–12271, doi:10.5194/acp-16-12239-2016, 2016.

Sheu, G.-R. and Lin, N.-H.: Characterizations of wet mercury deposition to a remote islet (Pengjiayu) in the subtropical Northwest Pacific Ocean, Atmos. Environ., 77, 474–481, doi:10.1016/j.atmosenv.2013.05.038, 2013.

Sigha-Nkamdjou, L., Galy-Lacaux, C., Pont, V., Richard, S., Sighomnou, D. and Lacaux, J. P.: Rainwater Chemistry and Wet Deposition over the Equatorial Forested Ecosystem of Zoétélé (Cameroon), J. Atmos. Chem., 46(2), 173–198, doi:10.1023/A:1026057413640, 2003.

Simon, S., Klemm, O., Tarek, E.-M., Joschka, W., Katharina, A., Po-Hsiung, L., Shih-Chieh, C., Neng-Huei, L., Guenter, E., Shih-Chieh, H., Tsong-Huei, W., Ya-Nan, W. and Yu-Chi, L.: Chemical Composition of Fog Water at Four Sites in Taiwan, Aerosol Air Qual. Res., 16(3), 618–631, doi:10.4209/aaqr.2015.03.0154, 2016.

Simpson, D., Benedictow, A., Berge, H., Bergström, R., Emberson, L. D., Fagerli, H., Flechard, C. R., Hayman, G. D., Gauss, M., Jonson, J. E., Jenkin, M. E., Nyíri, A., Richter, C., Semeena, V. S., Tsyro, S., Tuovinen, J.-P., Valdebenito, Á. and Wind, P.: The EMEP MSC-W chemical transport model–technical description, Atmos. Chem. Phys., 12(16), 7825–7865, doi:10.5194/acp-12-7825-2012, 2012.

Søvde, O. A., Prather, M. J., Isaksen, I. S. A., Berntsen, T. K., Stordal, F., Zhu, X., Holmes, C. D. and Hsu, J.: The chemical transport model Oslo CTM3, Geosci. Model Dev., 5(6), 1441–1469, doi:10.5194/gmd-5-1441-2012, 2012.

Stavrakou, T., Müller, J.-F., Peeters, J., Razavi, A., Clarisse, L., Clerbaux, C., Coheur, P.-F., Hurtmans, D., De Mazière, M., Vigouroux, C., Deutscher, N. M., Griffith, D. W. T., Jones, N. and Paton-Walsh, C.: Satellite evidence for a large source of formic acid from boreal and tropical forests, Nat. Geosci., 5(1), 26–30, doi:10.1038/ngeo1354, 2012.

Stettler, M. E. J., Eastham, S. and Barrett, S. R. H.: Air quality and public health impacts of UK airports. Part I: Emissions, Atmos. Environ., 45(31), 5415–5424, doi:10.1016/j.atmosenv.2011.07.012, 2011.

Straub, D. J., Lee, T. and Collett Jr., J. L.: Chemical composition of marine stratocumulus clouds over the eastern Pacific Ocean, J. Geophys. Res. Atmospheres, 112(D4), doi:10.1029/2006JD007439, 2007.

Stumm, Werner., Sigg, Laura. and Schnoor, J. L.: Aquatic chemistry of acid deposition, Environ. Sci. Technol., 21(1), 8–13, doi:10.1021/es00155a001, 1987.

Sun, L., Wang, Y., Yue, T., Yang, X., Xue, L. and Wang, W.: Evaluation of the behavior of clouds in a region of severe acid rain pollution in southern China: species, complexes, and variations, Environ. Sci. Pollut. Res., 22(18), 14280–14290, doi:10.1007/s11356-015-4674-5, 2015.

Sun, M., Wang, Y., Wang, T., Fan, S., Wang, W., Li, P., Guo, J. and Li, Y.: Cloud and the corresponding precipitation chemistry in south China: Water-soluble components and pollution transport, J. Geophys. Res., 115(D22), doi:10.1029/2010JD014315, 2010.

Talbot, R. W., Andreae, M. O., Berresheim, H., Jacob, D. J. and Beecher, K. M.: Sources and sinks of formic, acetic, and pyruvic acids over central Amazonia: 2. Wet season, J. Geophys. Res., 95(D10), 16799, doi:10.1029/JD095iD10p16799, 1990.

Talbot, R. W., Dibb, J. E., Lefer, B. L., Scheuer, E. M., Bradshaw, J. D., Sandholm, S. T., Smyth, S., Blake, D. R., Blake, N. J., Sachse, G. W., Collins, J. E. and Gregory, G. L.: Large-scale distributions of tropospheric nitric, formic, and acetic acids over the western Pacific basin during wintertime, J. Geophys. Res. Atmospheres, 102(D23), 28303–28313, doi:10.1029/96JD02975, 1997.

Tost, H., Jöckel, P., Kerkweg, A., Pozzer, A., Sander, R. and Lelieveld, J.: Global cloud and precipitation chemistry and wet deposition: tropospheric model simulations with ECHAM5/MESSy1, Atmos. Chem. Phys., 7(10), 2733–2757, doi:10.5194/acp-7-2733-2007, 2007.

Travis, K. R., Jacob, D. J., Fisher, J. A., Kim, P. S., Marais, E. A., Zhu, L., Yu, K., Miller, C. C., Yantosca, R. M., Sulprizio, M. P., Thompson, A. M., Wennberg, P. O., Crounse, J. D., St. Clair, J. M., Cohen, R. C., Laughner, J. L., Dibb, J. E., Hall, S. R., Ullmann, K., Wolfe, G. M., Pollack, I. B., Peischl, J., Neuman, J. A. and Zhou, X.: Why do models overestimate surface ozone in the Southeast United States?, Atmos. Chem. Phys., 16(21), 13561–13577, doi:10.5194/acp-16-13561-2016, 2016.

U.S. Environmental Protection Agency: 2011 National Emissions Inventory (NEI) Data, [online] Available from: https://www.epa.gov/air-emissions-inventories/2011-national-emissions-inventory-nei-data (Accessed 23 March 2018), 2018.

van Pinxteren, D., Fomba, K. W., Mertes, S., Müller, K., Spindler, G., Schneider, J., Lee, T., Collett, J. L. and Herrmann, H.: Cloud water composition during HCCT-2010: Scavenging efficiencies, solute concentrations, and droplet size dependence of inorganic ions and dissolved organic carbon, Atmos. Chem. Phys., 16(5), 3185–3205, doi:10.5194/acp-16-3185-2016, 2016.

Venkatram, A., Karamchandani, P. K. and Misra, P. K.: Testing a comprehensive acid deposition model, Atmos. Environ. 1967, 22(4), 737–747, doi:10.1016/0004-6981(88)90011-X, 1988.

Vet, R., Artz, R. S., Carou, S., Shaw, M., Ro, C.-U., Aas, W., Baker, A., Bowersox, V. C., Dentener, F., Galy-Lacaux, C., Hou, A., Pienaar, J. J., Gillett, R., Forti, M. C., Gromov, S., Hara, H., Khodzher, T., Mahowald, N. M., Nickovic, S., Rao, P. S. P. and Reid, N. W.: A global assessment of precipitation chemistry and deposition of sulfur, nitrogen, sea salt, base cations, organic acids, acidity and pH, and phosphorus, Atmos. Environ., 93, 3–100, doi:10.1016/j.atmosenv.2013.10.060, 2014.

Vinken, G. C. M., Boersma, K. F., Jacob, D. J. and Meijer, E. W.: Accounting for non-linear chemistry of ship plumes in the GEOS-Chem global chemistry transport model, Atmos. Chem. Phys., 11(22), 11707–11722, doi:10.5194/acp-11-11707-2011, 2011.

Vong, R. J., Baker, B. M., Brechtel, F. J., Collier, R. T., Harris, J. M., Kowalski, A. S., McDonald, N. C. and Mcinnes, L. M.: Ionic and trace element composition of cloud water collected on the Olympic Peninsula of Washington State, Atmos. Environ., 31(13), 1991–2001, doi:10.1016/S1352-2310(96)00337-8, 1997.

Wang, C., Corbett, J. J. and Firestone, J.: Improving Spatial Representation of Global Ship Emissions Inventories, Environ. Sci. Technol., 42(1), 193–199, doi:10.1021/es0700799, 2008.

Wang, Q., Jacob, D. J., Fisher, J. A., Mao, J., Leibensperger, E. M., Carouge, C. C., Le Sager, P., Kondo, Y., Jimenez, J. L., Cubison, M. J. and Doherty, S. J.: Sources of carbonaceous aerosols and deposited black carbon in the Arctic in winter-spring: implications for radiative forcing, Atmos. Chem. Phys., 11(23), 12453–12473, doi:10.5194/acp-11-12453-2011, 2011.

Wang, W., Xu, W., Collett, J. L., Liu, D., Zheng, A., Dore, A. J. and Liu, X.: Chemical compositions of fog and precipitation at Sejila Mountain in the southeast Tibetan Plateau, China, Environ. Pollut., 253, 560–568, doi:10.1016/j.envpol.2019.07.055, 2019.

Wang, X., Jacob, D. J., Eastham, S. D., Sulprizio, M. P., Zhu, L., Chen, Q., Alexander, B., Sherwen, T., Evans, M. J., Lee, B. H., Haskins, J. D., Lopez-Hilfiker, F. D., Thornton, J. A., Huey, G. L. and Liao, H.: The role of chlorine in global tropospheric chemistry, Atmos. Chem. Phys., 19(6), 3981–4003, doi:10.5194/acp-19-3981-2019, 2019.

Wang, Y., Jacob, D. J. and Logan, J. A.: Global simulation of tropospheric O_3-NOx-hydrocarbon chemistry: 1. Model formulation, J. Geophys. Res. Atmospheres, 103(D9), 10713–10725, doi:10.1029/98JD00158, 1998.

Wang, Z., Sorooshian, A., Prabhakar, G., Coggon, M. M. and Jonsson, H. H.: Impact of emissions from shipping, land, and the ocean on stratocumulus cloud water elemental composition during the 2011 E-PEACE field campaign, Atmos. Environ., 89, 570–580, doi:10.1016/j.atmosenv.2014.01.020, 2014.

Warneck, P.: Chapter 8 Chemistry of clouds and precipitation, in International Geophysics, vol. 71, pp. 451–510, Elsevier., 2000.

Watanabe, K., Honoki, H., Iwai, A., Tomatsu, A., Noritake, K., Miyashita, N., Yamada, K., Yamada, H., Kawamura, H. and Aoki, K.: Chemical Characteristics of Fog Water at Mt. Tateyama, Near the Coast of the Japan Sea in Central Japan, Water. Air. Soil Pollut., 211(1–4), 379–393, doi:10.1007/s11270-009-0307-2, 2010.

Watanabe, S., Hajima, T., Sudo, K., Nagashima, T., Takemura, T., Okajima, H., Nozawa, T., Kawase, H., Abe, M., Yokohata, T., Ise, T., Sato, H., Kato, E., Takata, K., Emori, S. and Kawamiya, M.: MIROC-ESM 2010: model description and basic results of CMIP5-20c3m experiments, Geosci. Model Dev., 4(4), 845–872, doi:10.5194/gmd-4-845-2011, 2011.

Watmough, S. A., Aherne, J., Alewell, C., Arp, P., Bailey, S., Clair, T., Dillon, P., Duchesne, L., Eimers, C., Fernandez, I., Foster, N., Larssen, T., Miller, E., Mitchell, M. and Page, S.: Sulphate, Nitrogen and Base Cation Budgets at 21 Forested Catchments in Canada, the United States and Europe, Environ. Monit. Assess., 109(1–3), 1–36, doi:10.1007/s10661-005-4336-z, 2005.

Weathers, K. C., Likens, G. E., Bormann, F. Herbert., Bicknell, S. H., Bormann, B. T., Daube, B. C., Eaton, J. S., Galloway, J. N., Keene, W. C. and et al., .: Cloudwater chemistry from ten sites in North America, Environ. Sci. Technol., 22(9), 1018–1026, doi:10.1021/es00174a004, 1988.

van der Werf, G. R., Randerson, J. T., Giglio, L., van Leeuwen, T. T., Chen, Y., Rogers, B. M., Mu, M., van Marle, M. J. E., Morton, D. C., Collatz, G. J., Yokelson, R. J. and Kasibhatla, P. S.: Global fire emissions estimates during 1997–2016, Earth Syst. Sci. Data, 9(2), 697–720, doi:10.5194/essd-9-697-2017, 2017.

Wesely, M.: Parameterization of surface resistances to gaseous dry deposition in regional-scale numerical models, Atmos. Environ. 1967, 23(6), 1293–1304, doi:10.1016/0004-6981(89)90153-4, 1989.

Xu, G., Lee, X., Lü, Y., Chen, Y. and Huang, D.: Seasonal variations of carboxylic acids and their contributions to the rainwater acidity: A case study of Guiyang and Shangzhong, China, Chin. Sci. Bull., 55(16), 1667–1673, doi:10.1007/s11434-009-3343-9, 2010.

Yoboué, V., Galy-Lacaux, C., Lacaux, J. P. and Silué, S.: Rainwater Chemistry and Wet Deposition over the Wet Savanna Ecosystem of Lamto (Côte d'Ivoire), J. Atmos. Chem., 52(2), 117–141, doi:10.1007/s10874-005-0281-z, 2005.

Zheng, B., Tong, D., Li, M., Liu, F., Hong, C., Geng, G., Li, H., Li, X., Peng, L., Qi, J., Yan, L., Zhang, Y., Zhao, H., Zheng, Y., He, K. and Zhang, Q.: Trends in China's anthropogenic emissions since 2010 as the consequence of clean air actions, Atmos. Chem. Phys., 18(19), 14095–14111, doi:10.5194/acp-18-14095-2018, 2018.

Zhu, C., Chen, J., Wang, X., Li, J., Wei, M., Xu, C., Xu, X., Ding, A. and Collett, J. L.: Chemical Composition and Bacterial Community in Size-Resolved Cloud Water at the Summit of Mt. Tai, China, Aerosol Air Qual. Res., 18(1), 1–14, doi:10.4209/aaqr.2016.11.0493, 2018.

Zinder, B., Schumann, T. and Waldvogel, A.: Aerosol and hydrometeor concentrations and their chemical composition during winter precipitation along a mountain slope—II. Enhancement of below-cloud scavenging in a stably stratified atmosphere, Atmos. Environ. 1967, 22(12), 2741–2750, doi:10.1016/0004-6981(88)90441-6, 1988.

Table 1: Henry's law coefficients for the calculations of cloudwater and ~~rainwater~~ precipitation pH[a]

Species	H (M atm^{-1}) at 298 K	$\frac{d \ln H}{d(1/T)}$ (K)
HNO$_3$	2.1×10^5	0
HCl	1.5×10^3	2300
NH$_3$	60	4200
HCOOH	8.8×10^3	6100
CH$_3$COOH	4.0×10^3	6300
SO$_2$	1.2	3100
CO$_2$	3.4×10^{-2}	2400

[a] From the compilation of Sander (2015).

Table 2: Acid/base dissociation constants for the calculations of cloudwater and ~~rainwater~~precipitation pH[a]

Equilibrium reactions	K (M or M^2) at 298 K	$\frac{d \ln K}{d(1/T)}$ (K)
$HNO_3\,(aq) \leftrightarrow H^+ + NO_3^-$	15	8700
$HCl\,(aq) \leftrightarrow H^+ + Cl^-$	1.7×10^6	6900
$NH_4OH\,(aq) \leftrightarrow NH_4^+ + OH^-$	1.7×10^{-5}	-450
$HCOOH\,(aq) \leftrightarrow H^+ + HCOO^-$	1.8×10^{-4}	150
$CH_3COOH\,(aq) \leftrightarrow H^+ + CH_3COO^-$	1.7×10^{-5}	50
$SO_2 \cdot H_2O \leftrightarrow H^+ + HSO_3^-$	1.3×10^{-2}	2000
$HSO_3^- \leftrightarrow H^+ + SO_3^{2-}$	6.6×10^{-8}	1500
$CO_2 \cdot H_2O \leftrightarrow H^+ + HCO_3^-$	4.3×10^{-7}	-1000
$HCO_3^- \leftrightarrow H^+ + CO_3^{2-}$	4.7×10^{-11}	-1800
$H_2O \leftrightarrow H^+ + OH^-$	1×10^{-14}	-6700
$CaCO_3(s) \leftrightarrow Ca^{2+} + CO_3^{2-}$	3.3×10^{-9}	-1200

[a] From Pandis and Seinfeld (1989), except for $CaCO_3(s)$ (Nordstrom et al., 1990), and $HCOOH(aq)$ and $CH_3COOH(aq)$ (Khare et al., 1999).

Table 3: Species included in the cloudwater pH calculation[a]

Conserved totals ≡ Sum of partitioned species
$H_2SO_{4,T} \equiv SO_4^{2-}$ [b]
$HNO_{3,T} \equiv HNO_3(g) + HNO_3(aq) + NO_3^-$
$HCl_T \equiv HCl(g) + HCl(aq) + Cl^-$
$NH_{3,T} \equiv NH_3(g) + NH_4OH(aq) + NH_4^+$
$HCOOH_T \equiv HCOOH(g) + HCOOH(aq) + HCOO^-$
$CH_3COOH_T \equiv CH_3COOH(g) + CH_3COOH(aq) + CH_3COO^-$
$SO_{2,T} \equiv SO_2(g) + SO_2(aq) + HSO_3^- + SO_3^{2-}$
$CO_{2,T} \equiv CO_2(g) + CO_2(aq) + HCO_3^- + CO_3^{2-}$ [c]
$Ca_T \equiv Ca^{2+} + CaCO_3(s)$
$Na_T \equiv Na^+$

[a] The calculation assumes a closed system for the cloudy fraction of the model grid cell where concentration totals (T) are conserved and are partitioned between species using the Henry's law and acid-base dissociation equilibria of Tables 1 and 2, and the local cloudwater liquid water content and temperature.

[b] H_2SO_4 has sufficiently low vapor pressure to be completely in the cloudwater phase, and $H_2SO_4(aq)$ and HSO_4^- concentrations are negligible at typical cloudwater pH (> 3).

[c] $CO_2(g)$ mixing ratio is taken to be 390 ppm as representative of 2013.

HCOOH wet deposition flux

Observed: 6.9; GEOS-Chem: 7.5

CH₃COOH wet deposition flux

Observed: 5.7; GEOS-Chem: 1.5
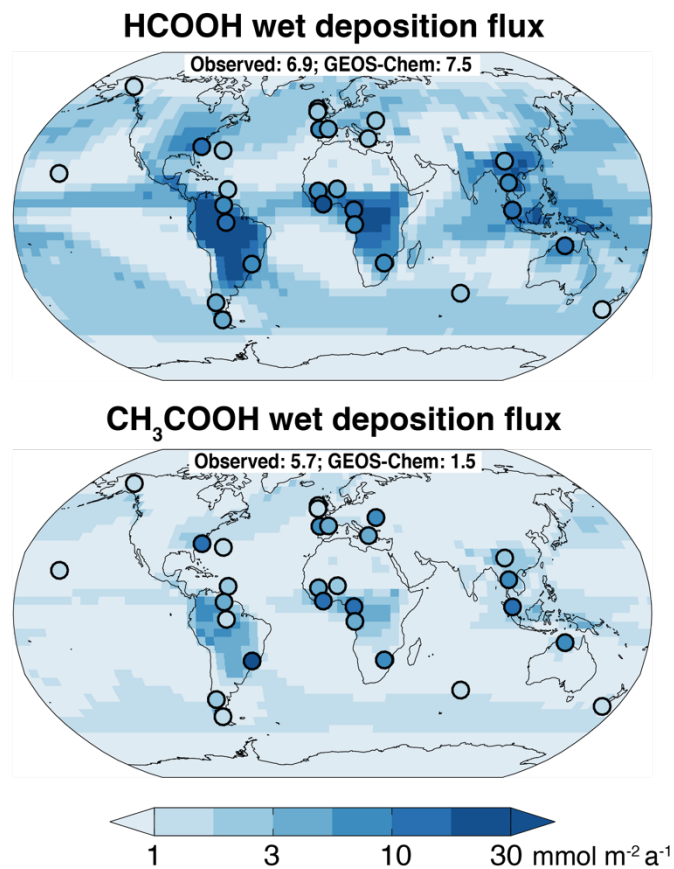
1   3   10   30 mmol m⁻² a⁻¹

Figure 1: Annual mean wet deposition fluxes of HCOOH and CH₃COOH. The GEOS-Chem model values (contours) are for the year 2013 and the observations (circles) are for various years as compiled by Vet et al. (2014) and Keene et al. (2015). The compilations only include studies that used adequate methods to preserve HCOOH and CH₃COOH in ~~rainwater~~precipitation samples. We exclude studies with measurement periods of less than a year. For studies that reported only ~~rainwater~~precipitation concentrations, we estimate the deposition fluxes using climatological rainfall data for the corresponding locations from the Global Precipitation Climatology Center (Meyer-Christoffer et al., 2018). The global mean observed fluxes and the corresponding GEOS-Chem fluxes are shown inset.

Global distribution of cloudwater pH
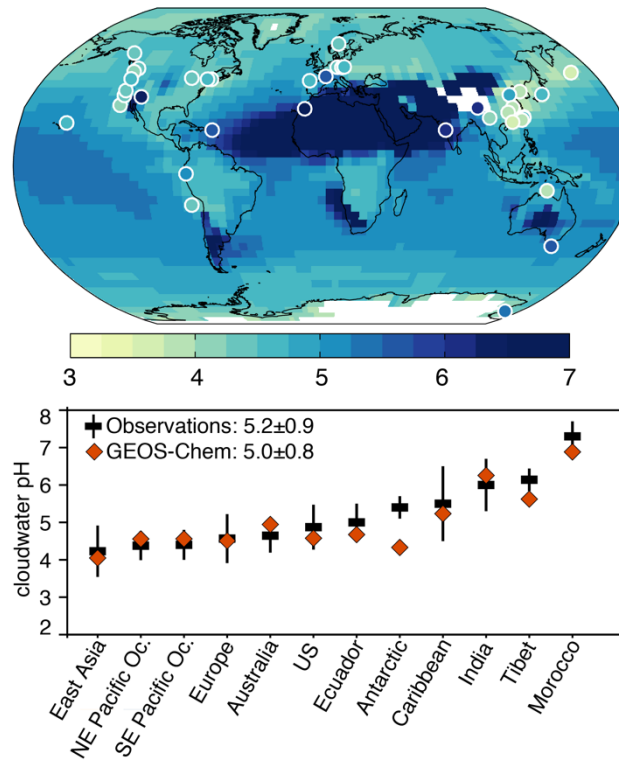
Figure 2: Observed and simulated cloudwater pH. The top panel shows the GEOS-Chem annual mean cloudwater pH below 700 hPa for the year 2013 along with cloudwater pH observations (filled circles) collected since 1980 (Table A1). See Sect. 2.3 for the procedure to compute average pH in the model. White color denotes areas where the topographic elevation is higher than 700 hPa. The maximum modeled and observed pH values are 8.2 and 7.3, respectively. The bottom panel shows the observations grouped by regions (Table A1), with means ± standard deviations calculated from the ensemble of data sets for the region, and the corresponding GEOS-Chem mean values sampled at the location and month of the measurements. The global mean ± standard deviation pH values computed from the regional mean observed and modeled values are inset in the bottom panel.
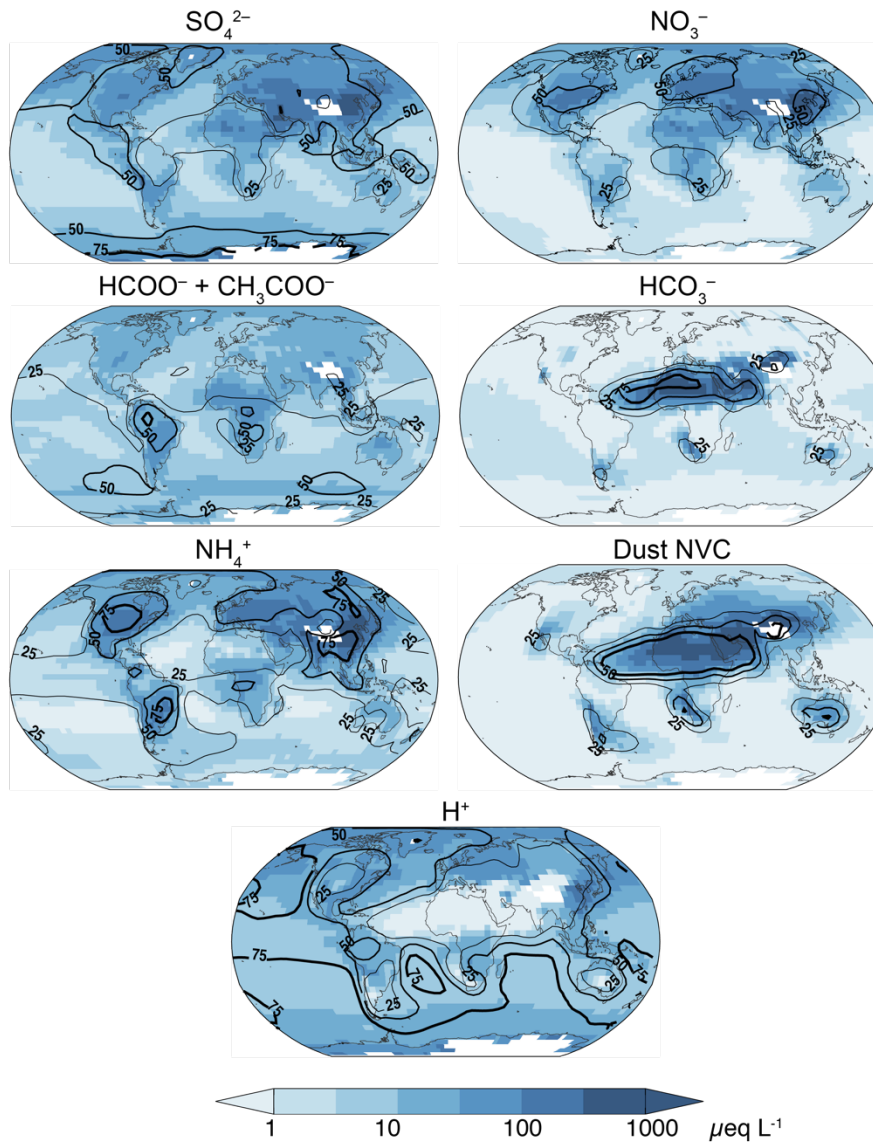
Figure 3: GEOS-Chem cloudwater equivalent concentrations of major acidic and basic ions. Values are annual volume weighted averages below 700 hPa for the year 2013. The contour lines (25%, 50%, 75%) show the percent contribution of each ion to the total anion or cation equivalents. Na$^+$ and Cl$^-$ are not included in this total because they are largely in balance and make little net contribution to acidity. White color denotes areas where the topographic elevation is higher than 700 hPa.
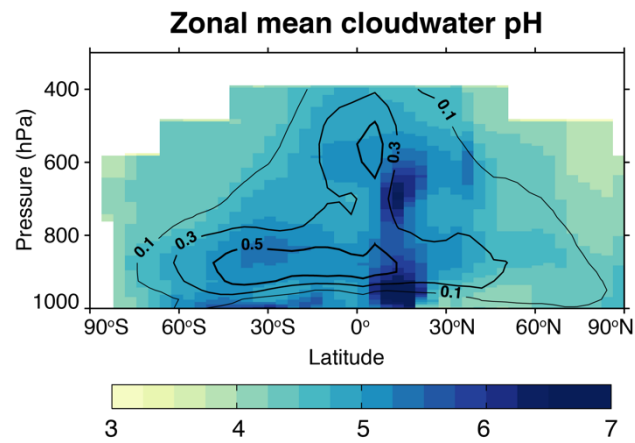
Figure 4: Zonal mean cloudwater pH simulated by GEOS-Chem. Values are annual volume weighted averages for the year 2013. The contour lines show the annual mean MERRA-2 cloud liquid water content in g m^{-3} for the cloudy fraction of grid cells where a liquid cloud is present. White color denotes areas where the cloud liquid water content is below 0.01 g m^{-3}.

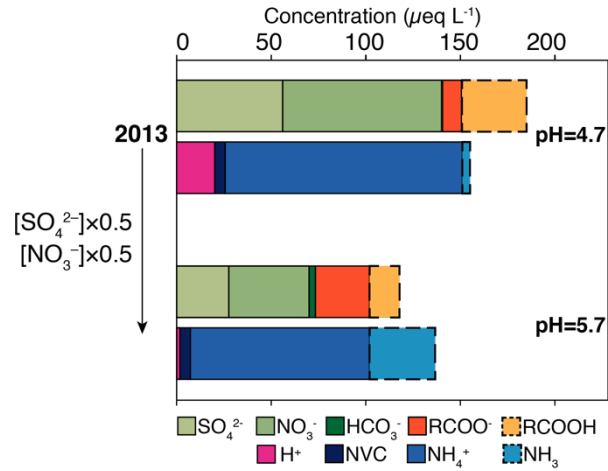**Cloudwater pH sensitivity to reduced acid inputs**

Figure 5: Sensitivity of cloudwater pH to decreasing acid inputs over the contiguous US. The upper bars show the volume weighted average concentrations of acidic and basic ions for 2013, with additional dashed lines showing the undissociated concentrations of carboxylic acids (RCOOH) and the gas-phase concentration of ammonia (NH₃). The lower bars show the effect of decreasing [SO₄²⁻] and [NO₃⁻] by half relative to 2013 levels. All concentrations are expressed as cloudwater equivalents. The corresponding pH values are indicated.
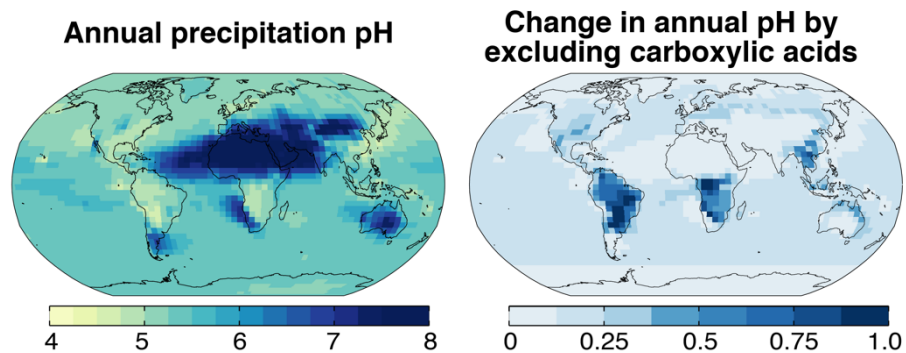
Annual precipitation pH

Change in annual pH by excluding carboxylic acids

Figure 6: Annual mean ~~rainwater~~precipitation pH simulated by GEOS-Chem for 2013. The right panel shows the change in ~~rainwater~~precipitation pH when [HCOO⁻] and [CH₃COO⁻] are excluded from the ionic charge balance. ~~Rainwater as defined here includes snow as well as rain.~~ See Sect. 2.3 for the procedure to compute average pH in the model.
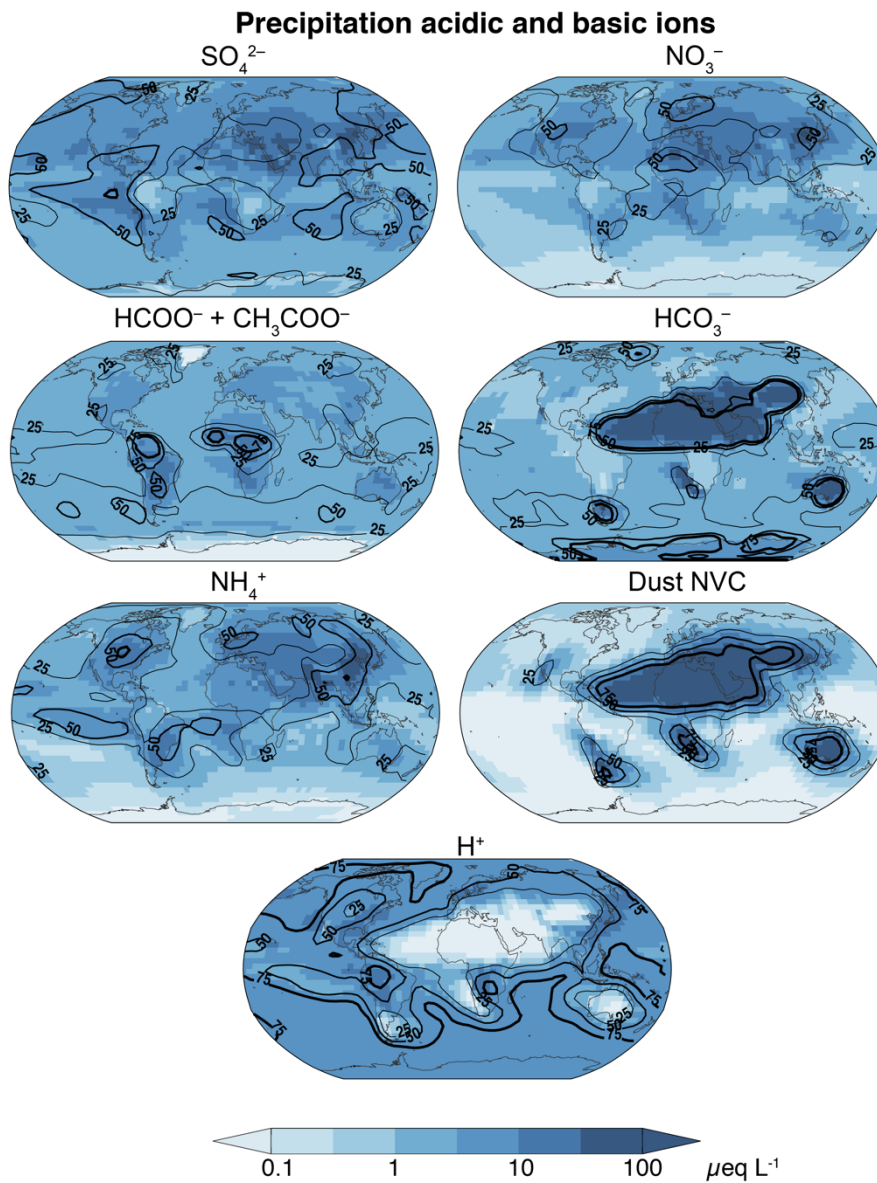
Figure 7: GEOS-Chem ~~rainwater~~precipitation **equivalent concentrations of major acidic and basic ions for the year 2013. The contour lines (25%, 50%, 75%) show the percent contribution of each ion to the total anion or cation equivalents. Na^+ and Cl^- are not included in this total because they are largely in balance and make little net contribution to acidity.**
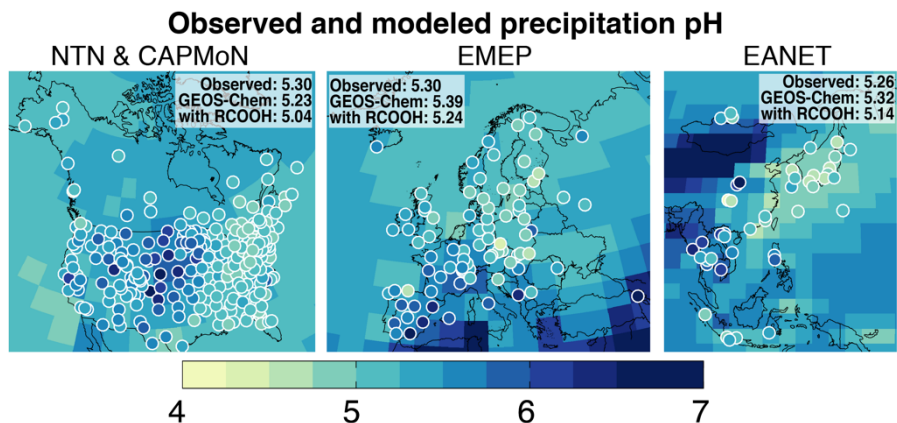
Figure 8: Annual volume weighted average (VWA) ~~rainwater~~precipitation pH over North America, Europe and East Asia for the year 2013. Values are the precipitation volume weighted averages of the monthly means (Eq. 6). The GEOS-Chem model values (solid background) exclude RCOOH (HCOOH and CH$_3$COOH) in the pH calculation for comparison to observations. Observations (circles) are from the US National Trends Network (NTN), the Canadian Air and Precipitation Monitoring Network (CAPMoN), the European Monitoring and Evaluation Programme (EMEP), and the Acid Deposition Monitoring Network in East Asia (EANET). The EANET sites in Malaysia are not shown because of their different sampling procedure (see text). The insets in each panel show the spatial means of the observations for the corresponding region together with the corresponding GEOS-Chem means at the measurement locations. The mean GEOS-Chem pH values with RCOOH included in the pH calculations are also shown.

Acidic wet depostion flux to ecoystems
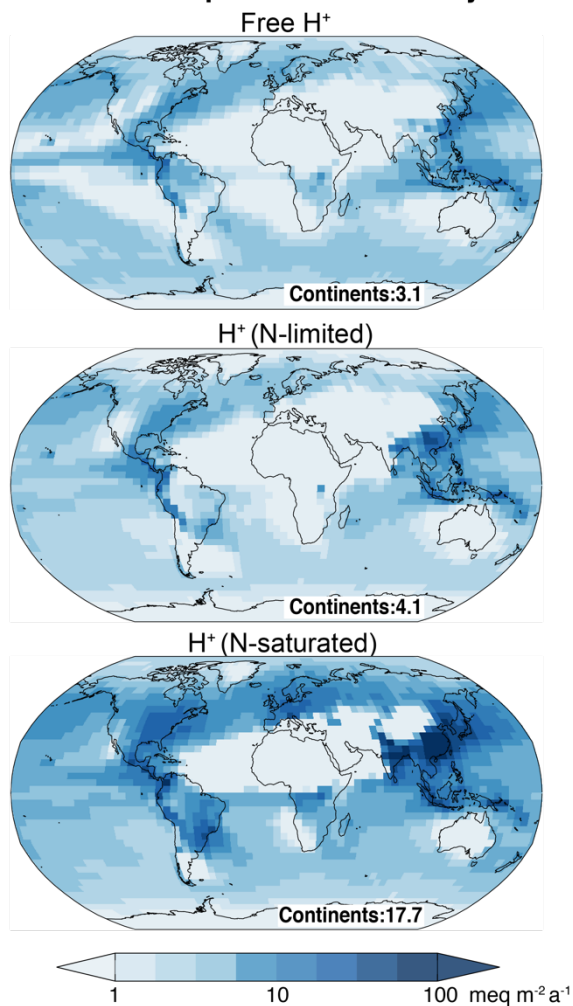
Figure 9: Acid wet deposition fluxes including post-depositional effects. Values are annual means for 2013 as simulated by GEOS-Chem. H^+ associated with carboxylic acids is excluded as these acids are rapidly consumed by bacteria. The free H^+ flux represents the direct H^+ input to ecosystems not accounting for any post-deposition nitrogen (N) transformation. The H^+ flux for N-limited conditions is computed using Eq. (7) and assumes complete assimilation of NO_3^- and NH_4^+, while the H^+ flux for N-saturated conditions is computed using Eq. (8) and assumes complete nitrification of NH_4^+ and no assimilation of NO_3^-. The global mean flux over continents in units of meq m^{-2} a^{-1} is indicated.

Appendix

Table A1: Cloudwater pH observations grouped by region and listed from west to east and north to south.

Location	Altitude (km)	Period	Mean ± std dev	Median	Range	Reference
NE Pacific Ocean						
California coast 29-33N; 121-123W	0–1	Jul, 2001	4±0.4 [a, b]	4	3.3–4.8	Straub et al. (2007)
California coast 35-37N; 122-123W [a]	0.12–0.8	Jul–Aug, 2011	4.5±0.7	-	-	Z. Wang et al. (2014)
California coast 34-43N; 119-126W	0.12–1	Jul–Aug, 2013	4.3±0.5	-	-	Prabhakar et al. (2014)
Hawaii 22N; 152W	0–1	Jun, 1980	4.5±0.1 [a, c]	-	4.2–4.7	Parungo et al. (1982)
Alaska, US 58N; 135W	0.8	Aug–Sep, 1984; July–Aug, 1985	4.5±0.4	4.8	-	Bormann et al. (1989)
Whistler Mtn, Canada, 50N;123N	1.7	Jun–Jul, 2010	4.4 [b]	4.4	-	Ervens et al. (2013)
Cheeka Peak, US, 48N; 125W	1	May, 1993	4.2±0.2	-	-	Vong et al. (1997)
Mary's Peak, US, 45N; 124W	1.3	Jul–Nov, 1985	4.7±0.3 [a]	5.2	4.4-4.9	Bormann et al. (1989)
Continental United States						
Mt. Washington 44N; 71W	1.9	Jun–Aug, 2008–2010	4.3	-	-	G. Murray et al. (2013)
Whiteface Mountain 44N; 74W	1.5	Jun–Sep, 2010–2013	4.5±0.8 [a]	-	3.4-6.6	Schwab et al. (2016)
Michigan 44-46N; 83-85W	1.4–3.1	Jul–Aug, 2005	4.4±0.8 [a]	-	2.2-5.2	Hill et al. (2007); Pye et al. (2020)
Mt. Elders 35N; 112W	2.8	Jun–Sep, 2005–2007	6.3±0.4 [a]	-	5.1-6.6	Hutchings et al. (2009)
Caribbean						
Puerto Rico 18N; 65W	1.1	2004–2007	5.5±1.0	-	-	Gioda et al.(2011)
Southeast Pacific Ocean						
Peru/Chile coast 16-24S; 72-82W	0–1	Oct–Nov,2008	4.4±0.4 [a]	-	3.5-6	Benedict et al. (2012)

Location	Altitude (km)	Period	Mean ± std dev	Median	Range	Reference
Ecuador						
Andes 79W; 4S	1.9–3.2	2004–2009	5.0±0.5 [a]	-	-	Makowski Giannoni et al. (2013, 2016); Pye et al. (2020)
Europe						
Åreskutan, Sweden, 63N; 13E	1.3	Jul–Aug, 1983; Jul–Aug, 1984	4.4	-	-	Ogren & Rodhe (1986)
Mt. Schmucke, Germany, 51N; 11E	0.9	Sep–Oct, 2010	4.3±0.4 [a]	4.6	3.6–5.3	van Pinxteren et al. (2016)
Mt. Milesovka, Czech Rep., 51N; 14E	0.8	May–June 2006	4.1±0.2 [a]	-	3.8–4.7	Fisak et al. (2009)
Mt. Szrenica, Poland, 51N; 16E	1.3	Dec, 2005 – Dec, 2006	4.6±1.0 [a]	-	3.5–7.4	Błaś et al. (2010)
Niesen, Switzerland, 47N; 7-8E	1.6–2.3	Apr–Oct, 2006; Apr–Oct 2007	6.5±0.5 [a]	-	5.8–7.7	Michna et al. (2015)
Puy de Dome, France, 46N; 3E	1.5	2001–2006; 2009–2011	5.5±1.1 [a]	5.6	3.1–7.6	Deguillaume et al. (2014)
Xistral Mountains, Spain, 44N; 8W	0.9	Sep, 2011–Apr 2012	4.5±0.4 [a]	-	3.8–5.2	Fernández-González et al. (2014)
Morocco						
Mt. Boutmezguida 29N; 10W	1.2	Nov–Jun, 2013–2015	7.3±0.4 [a]	-	7–8.5	Schunk et al. (2018); Pye et al. (2020)
India						
Sinhagad 18N; 74E	1.5	2007–2010	6.0±0.7 [a]	-	4.7–7.4	Budhavant et al. (2014)
Tibet						
Sejila mountain 30N; 95E	4	Jul, 2017–Sep, 2018	6.1±0.3	-	-	W. Wang et al. (2019)
East Asia						
North Pacific Ocean 45–51N,159–171E	0.1	Jul, 2012	3.6±0.2	-	-	H. Kim et al. (2019)
Yellow Sea 38N,125E	0.1	Jul, 2014	3.9±0.4 [a]	-	3.5–5	Boris et al. (2016); Pye et al. (2020)

Table A1 continued

Location	Altitude (km)	Period	Mean ± std dev	Median	Range	Reference
East Asia (contd.)						
Mt. Tateyama, Japan, 37N,138E	2.5	Sept–Oct, 2007–2009	4.5±0.7 [a]	-	3.5–6.3	K. Watanabe et al. (2010)
Mt. Tai, China, 36N; 117E	1.6	Jul–Oct, 2014	5.9±0.8 [a]	-	3.8–7.0	J. Li et al. (2017)
		Mar–Apr, June–July, Oct–Nov, 2007; Mar–Apr, Jun–Jul, 2008	4.3±1.3 [a]	-	2.6–7.6	Guo et al. (2012)
		Jun–Aug 2015	4.9±0.6 [a]	-	3.8–6.3	Zhu et al. (2018)
Mt. Lu, China, 30N; 116E	1.2	Aug–Sep, 2011; Mar–May, 2012	3.8±0.7 [a]	-	2.8–5.6	L. Sun et al. (2015)
Mt. Heng, China, 27N; 113E	1.3	Mar–May, 2009	3.8±1.0 [a]	-	2.9–6.9	M. Sun et al. (2010)
Ailaoshan, China, 25N; 101E	2.5	Dec 2015–Mar 2016	4.1±0.4 [a]	-	3.5–4.9	Nieberding et al. (2018)
Mt. Bamboo, Taiwan, 25N,122E	1.1	Jan–Mar 2009	4.1±0.6 [a]	-	3.1–5.6	Sheu & Lin (2013)
Chilan Mtn, Taiwan, 25N,122E	1.7	Apr–May, 2011	4.5±0.4 [a]	-	3.7–5.2	Simon et al. (2016)
Lulin Station, Taiwan, 23N,121E	2.9	Apr–May, 2011	3.9±0.3 [a]	-	3.4–4.5	Simon et al. (2016)
Mt. TaiMoSha, Hong Kong, 22N,114E	1	Oct–Nov 2016	3.6±0.7 [a]	-	3.0–6.0	Li et al. (2020)
Australia						
Cape Grim, 40-42S; 144-149E	0.6–1.5	Jun, 1981; Mar, 1983	5.5±0.5	-	-	Gillett & Ayers (1989)
Jabiru, 133E; 13S	2.7–3.7	Nov, 1985	3.8±0.4 [a]	-	3.5–5.2	Ayers & Gillett (1988)
Antarctic						
Antarctica coast 78S; 167E	0.6–1.5	Dec, 1982	5.4±0.3 [a]	-	4.9–6.2	Saxena & Lin (1990)

[a] Standard deviation estimated as range / 4.

[b] Median value used as the mean.

[c] Mean estimated as (max+min) / 2.